TECTONICS, VOL. 11, NO. 3, PAGES 634-662, JUNE 1992

THE TRANSANTARCTIC MOUNTAINS OF SOUTHERN VICTORIA LAND: THE APPLICATION OF APATITE FISSION TRACK ANALYSIS TO A RIFT SHOULDER UPLIFT

Paul G. Fitzgerald
Arizona State University, Department of Geology, Tempe

Abstract. A fission track study of the Transantarctic Mountains (TAM) in the Granite Harbour and Wilson Piedmont Glacier areas of southern Victoria Land reveals information on the timing of uplift, the amount of uplift and erosion, and the structure of the mountains, especially the onshore Transantarctic Mountain Front (TAM Front), which represents the boundary between East and West Antarctica. Apatite ages are <175 Ma and represent a thermal regime established after heating accompanying Jurassic magmatism. An apatite age profile from Mount England records a break in slope indicating uplift began at ~55 Ma. Horizontal sampling traverses, plus fieldwork, delineate the structure of the TAM Front as a zone of north-south striking, steeply dipping normal faults, with displacements, dominantly down to the east, of 40-1000 m. The overall structure of the mountains in the area studied can be envisaged as a large tilt block or flexure. Its westerly limb dips gently under the ice cap, compared to its faulted eastern edge, the TAM Front. The bounding structure to the south is the Ferrar fault and to the north is a graben through which the Mackay Glacier drains the polar plateau. The edge of the flexure, or axis of maximum uplift, lies at Mount Termination, ~30 km west of the McMurdo Sound coast. There has been ~6 km of uplift since the early Cenozoic and 4.5-5 km of erosion along this axis. The amount of uplift decreases to the west at the same rate as the decrease in dip of the Kukri Peneplain, but the amount of erosion decreases more quickly as indicated by the increasing height of the mountains to the west. The axis of maximum uplift is traced north to Granite Harbour. The axis does not parallel the coast but has a more northerly trend. North-south striking longitudinal faults that delineate the structure of the TAM Front lie at an acute angle to the axis, indicating a dextral component to the dominantly east-west extension in the Ross Embayment. Architecture of the TAM typifies the features of an upper plate passive mountain range, whereas the Ross Embayment has the characteristics of a lower plate. The TAM Front represents an upper plate breakaway zone. Transfer faults may exist up major outlet glaciers that cut the TAM. The inflection point in the coastline at the southern end of McMurdo Sound may be due to the presence of a major transfer fault up or near the Skelton Glacier.

INTRODUCTION

The Transantarctic Mountains (TAM) stretch from the Pacific Ocean side of Antarctica to the Atlantic Ocean (Figure 1) forming the morphological and geological boundary between East and West Antarctica [Dalziel et al., 1987]. East Antarctica is a remnant of Gondwana and consists dominantly of Precambrian rocks, whereas West Antarctica consists of at least four separate crustal blocks [Jankowski and Drewy, 1981], each with separate, and more recent histories than East Antarctica [Dalziel and Elliot, 1982]. The relationship between East and West Antarctica remains one of the outstanding problems in Antarctic geoscience, as does the uplift of the TAM themselves. Previous fission track work [Gleadow et al., 1984; Gleadow and Fitzgerald, 1987; Fitzgerald and Gleadow, 1988] has shown the uplift of the TAM to be a Cenozoic event, most likely associated with the subsidence and formation of the sedimentary basins of the adjacent Ross Embayment [Fitzgerald et al., 1986] and the sub-ice basins on the inland side of the TAM [Stern and ten Brink, 1989]. As such, the relationship of the TAM, an area of normal or slightly thickened continental crust [Bentley, 1983], to the Ross Embayment, an area of late Cretaceous(?) - Cenozoic extension and thinner continental crust [Cooper et al., 1987], indicates that the TAM are most likely a rift-margin uplift. The escarpment to this rift shoulder is perhaps most dramatically shown in the Royal Society Range where the mountains rise in excess of 4000 m elevation ~35 km from the coast.

Results from the Wilson Piedmont Glacier and Granite Harbour areas of southern Victoria Land emphasize the role of apatite fission track analysis in tectonic studies. The time of initiation of uplift of the TAM in this region is confirmed as early Cenozoic, and the structure of the Transantarctic Mountain Front (TAM Front) is defined as apatite fission track analysis is used to confirm the existence of suspected faults and constrain the displacements across these faults. These results are then discussed with regard to the formation of the TAM-Ross Embayment.

Geology of the Transantarctic Mountains

The TAM provide the most extensive rock outcrop anywhere in Antarctica (Figure 1). Precambrian and Cambrian metasediments together with Cambro-Ordovician granites of the Granite Harbour Intrusives and the Devonian Admiralty Intrusives form the basement rocks of the TAM. This basement was eroded to form a peneplain (the Kukri Peneplain) during the Ordovician-Silurian before being unconformably overlain by the now flat-lying or gently dipping shallow marine, glacial, and alluvial plain sediments of the Devonian-Triassic Beacon Supergroup. Jurassic tholeiitic magmatism is represented by sills of the Ferrar Dolerite in basement and cover rocks and by capping flows of the Kirkpatrick Basalt. The next recorded geological event in the TAM is late Cenozoic alkaline volcanism [Armstrong, 1978]. This was followed, at least in southern Victoria Land, by deposition of sediments of marine, nonmarine, lacustrine, and glacial origin [Torii, 1981; Webb et al., 1984]. Shallow drilling in the eastern Taylor Valley area of southern Victoria Land has cored sediments as old as early Miocene [Webb and Wrenn, 1982]. Offshore, drilling at Deep Sea Drilling Project site 270 in the central Ross Sea has identified sediments as old as late Oligocene [Hayes et al., 1975]. The oldest sediments cored in the Ross Sea region (early Oligocene, 33-38 Ma) have come from the CIROS-1 drill hole in McMurdo Sound, just offshore of the Dry Valleys [Barrett, 1987].

The TAM have been the site of repeated tectonism since the Precambrian. The Precambrian Beardmore Orogeny [Stump et al., 1991] as well as the Cambro-Ordovician Ross Orogeny have produced regional structures parallel or subparallel to the trend of the present TAM. Depositional basins of the Beacon

Paper Number 91TC02495.
0278-7407/92/91TC-02495$10.00

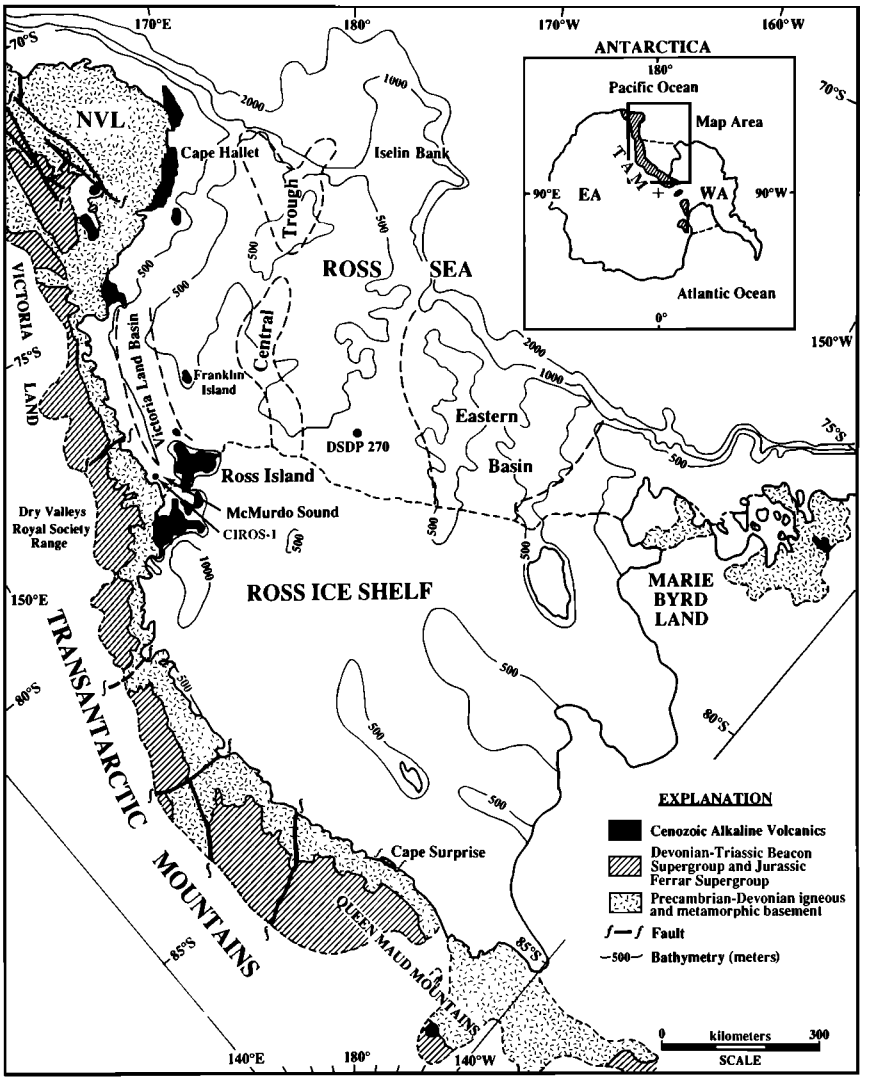

Fig. 1. Map of the Ross Embayment area showing the extent of the Transantarctic Mountains (TAM) and their position as the boundary between East (EA) and West Antarctica (WA). Onshore geology is modified from Craddock [1982], and the position of sedimentary basins of the Ross Sea is from Davey et al. [1983] and Cooper and Davey [1985]. Bathymetry is after Hayes and Davey [1975], Craddock [1982], and Robertson et al. [1982]. NVL is northern Victoria Land.

Supergroup were elongate along the trend of the TAM [Barrett, 1981], and exposed outcrops of the Jurassic tholeiitic magmatism also follow the line of the mountains [Kyle et al., 1981]. The present-day TAM would seem therefore to delineate a zone of fundamental crustal weakness that has been reactivated throughout geological history and at present marks the edge of the East Antarctic craton and the boundary with West Antarctica. However, the mountains themselves are not associated with a Cenozoic active plate margin, nor an active transform boundary, although some past transform motion in the Ross Embayment cannot be completely excluded [e.g., Davey, 1981; Grindley, 1981; Schmidt and Rowley, 1986].

The origin of the TAM has been debated since Priestley and David [1912] and David and Priestley [1914] suggested the mountains represent a "great horst" that is cut by transverse faults marked by the larger crosscutting glaciers. Table 1 tabulates the various papers that discuss the structure, uplift, and formation of the TAM.

Apatite Fission Track Analysis

It was realized some years ago that apatite ages get older with increasing elevation [Wagner and Reimer, 1972], and apatite fission track analysis is now routinely used to address geological problems associated with tectonics [e.g., Gleadow and Brooks, 1979; Naeser et al., 1983]. Recently, the use of confined track length measurements [e.g., Gleadow et al., 1986a, b], and a better understanding of annealing of fission tracks in apatite [Green et al., 1986; Laslett et al., 1987], has permitted development of forward modelling programs [Duddy et al., 1988; Green et al., 1989] that have allowed a better interpretation of apatite fission track data.

The observation that apatite ages increase with increasing elevation can be explained as the consequence of an idealized column of rock moving up through an idealized critical track retention isotherm (or closure temperature) during uplift and denudation leading to the formation of uplifted terrain. The

TABLE 1. Structure and Formation of the Transantarctic Mountains: Previous Ideas

	Reference
	Structure
The "Great Antarctic Horst"	Priestley and David [1912], David and Priestley [1914] Gould [1935]
Anticline	Hamilton [1960, 1963], Hamilton and Hayes [1960] Hamilton et al. [1965]
Monocline	King [1965]
Block faulting	Gunn and Warren [1962], Gunn and Walcott [1962] McKelvey and Webb [1962], Gunn [1963], Laird [1963] Grindley et al. [1964], Skinner [1964], McGregor [1965] Grindley [1967], Hamilton [1967], Murtaugh [1969] Skinner and Ricker [1968a, b], Calkin and Nichols [1972] Miagkov [1973], Katz [1982], Wrenn and Webb [1982]
associated with rifting	Haskell et al. [1965]
	Uplift and Formation
Upwarp of margin due to ice loading	Voronov [1964]
Ice loading causing mantle bulge	Grindley [1967]
Isostatic response	
underplating ??	Smithson [1972]
partial result of removal of rock by glaciation and its replacement by ice (Prince Charles Mountains analogy)	Wellman and Tingey [1981], Tingey [1985]
Phase changes	
polymorphic phase change at the base of the of the crust ("uplift began during the Jurassic")	Robinson [1964]
deep crustal phase changes due to delayed effects of the overriding by East Antarctica of anomalously hot asthenosphere formed under West Antarctica in the late Cretaceous (the anomalously hot asthenosphere having been brought closer to the surface by crustal stretching along the edge of the (modern) TAM).	Smith and Drewry [1984]
The TAM as a rift margin	Schopf [1969], Schmidt and Rowley [1986]
reactivated in the Cenozoic	Dalziel and Elliot [1982], Elliot [1985]
Glacial crustal bending and reheating	McGinnis et al. [1983]
Asymmetric extension: TAM as passive margin mountains, uplift of the TAM related to subsidence and formation of basins in the Ross Embayment due to asymmetric extension and the subsequent juxtaposition of crust and subcrustal lithosphere resulting in an isostatic response. Possible underplating also aids uplift.	Fitzgerald et al. [1986]
TAM supported by a broad flexure of the strong East Antarctic lithosphere. Thermal uplift associated with lateral heat conduction from the extended and thinned West Antarctic lithosphere. Also erosion and the Veining Meinesz uplift effect.	Stern and ten Brink [1989]
Petrologic data from lower crustal inclusions supports a thermally driven uplift for at least part of the uplift of the TAM.	Berg et al. [1989]

effective closure temperature, equivalent to the stage when approximately half the tracks become stable, actually varies with cooling rate [Wagner and Reimer, 1972; Dobson, 1973; Haack, 1977; Wagner et al., 1977]. For cooling rates of 0.1°-100°C m.y.$^{-1}$ over geologic time (periods of 10-100 m.y.) the effective track retention temperature is ~100° ±20°C [Naeser and Faul, 1969; Calk and Naeser, 1973; Harrison et al., 1979].

However, there has long been a realization that fission tracks anneal at all temperatures, and it is only the rate of annealing that varies with temperature. Studies of apatite age variation in deep drill holes [e.g., Naeser, 1981; Gleadow and Duddy, 1981] and annealing studies [e.g., Green et al., 1986; Laslett et al., 1987] show that apatite age decreases with depth (increasing temperature), forming a distinctive profile (Figure 2) until a

zero age is reached at a depth of 3-5 km (~110°C). The depth of zero apatite age will depend on the geothermal gradient, the duration of heating, and the chemical composition of the apatites [Green et al., 1986]. At temperatures near the base of the partial annealing zone (PAZ) the rate of annealing is almost instantaneous, but at surface temperatures it is very slow. Track length distributions will also vary with temperature and will form distinctive patterns depending on the temperature at which these samples have resided [Gleadow et al., 1986a, b]. Apatite ages may be meaningless in terms of dating geological events because they may have been modified by annealing. However, it is this characteristic of apatite fission track analysis that allows the thermal history (and hence tectonic history) of areas to be resolved [e.g., Green, 1986], especially when the variation of age and length over a vertical profile is examined [e.g., Fitzgerald and Gleadow, 1990; Brown, 1991].

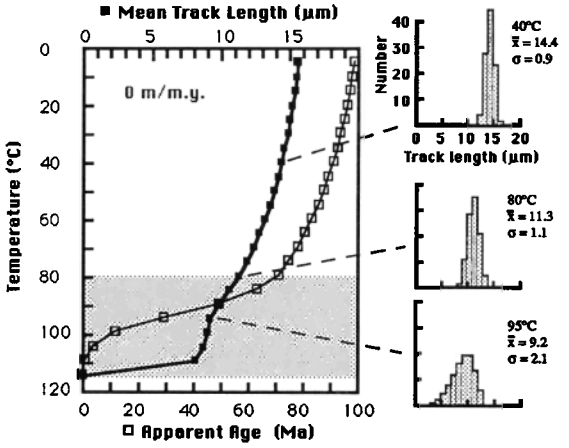

Fig. 2. Modelled variation of apparent apatite fission track ages and mean confined length with temperature determined using the annealing model (based on the annealing characteristics of Durango apatite) of Laslett et al. [1987] and Green et al. [1989] for a stable thermal and tectonic situation in which isotherms have remained static for 100 Ma. The stippled area is indicative of the area of most rapid annealing in the lower part of the partial annealing zone (PAZ). Modelled confined track length distributions (with mean lengths and standard deviations in microns) are shown for three temperatures, 40°C, 80°C, and 95°C.

SAMPLING STRATEGY AND FIELD EVIDENCE FOR FAULTING

Basement granitoid rocks from the Wilson Piedmont Glacier and the Granite Harbour areas of southern Victoria Land (Figure 3) were collected for apatite fission track analysis. The sampling strategy was tailored so that, at a number of localities, samples were taken from regular vertical intervals over a significant elevation range in order to reveal the most information about uplift. Elsewhere samples were taken on approximate transect lines across the trend of the TAM and across faults in order to reveal information on the structure of the mountains.

The Wilson Piedmont Glacier Area

The key area studied to define the structure of the TAM Front is along the Mount Doorly-Mount Allen ridge system (Figures 4 and 5). Results from a vertical profile collected from Mount Doorly and a preliminary cross section drawn from an aerial reconnaissance of this area have already been presented by Gleadow and Fitzgerald [1987], and the results presented herein confirm and extend the scope of that study.

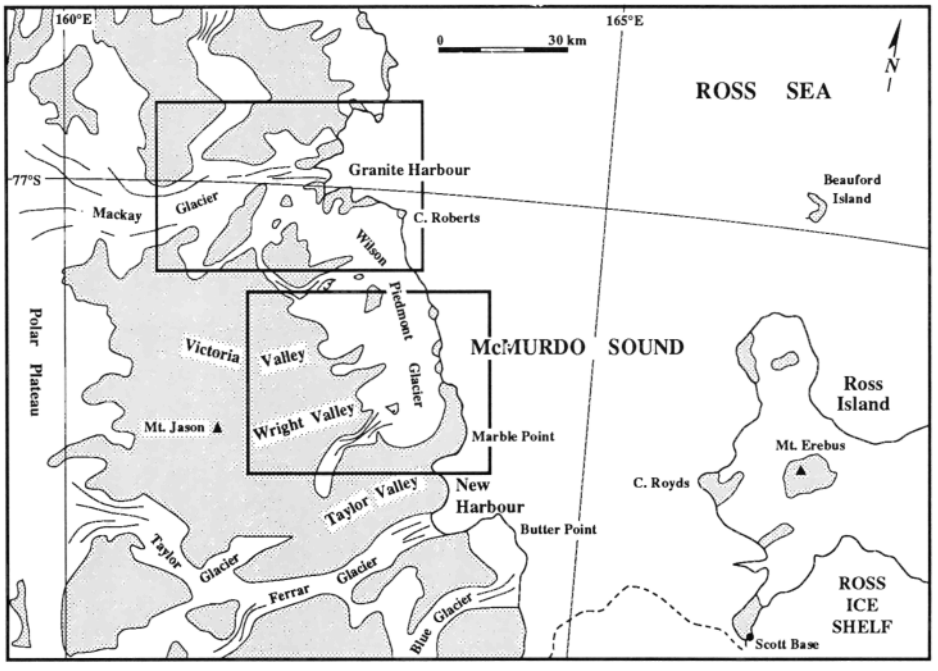

Fig. 3. Map of the Dry Valleys area in southern Victoria Land. The lower boxed area marks the position of Figures 4 and 11 in the Wilson Piedmont Glacier area, and the upper boxed area shows the position of Figures 7 and 13 in the Granite Harbour region.

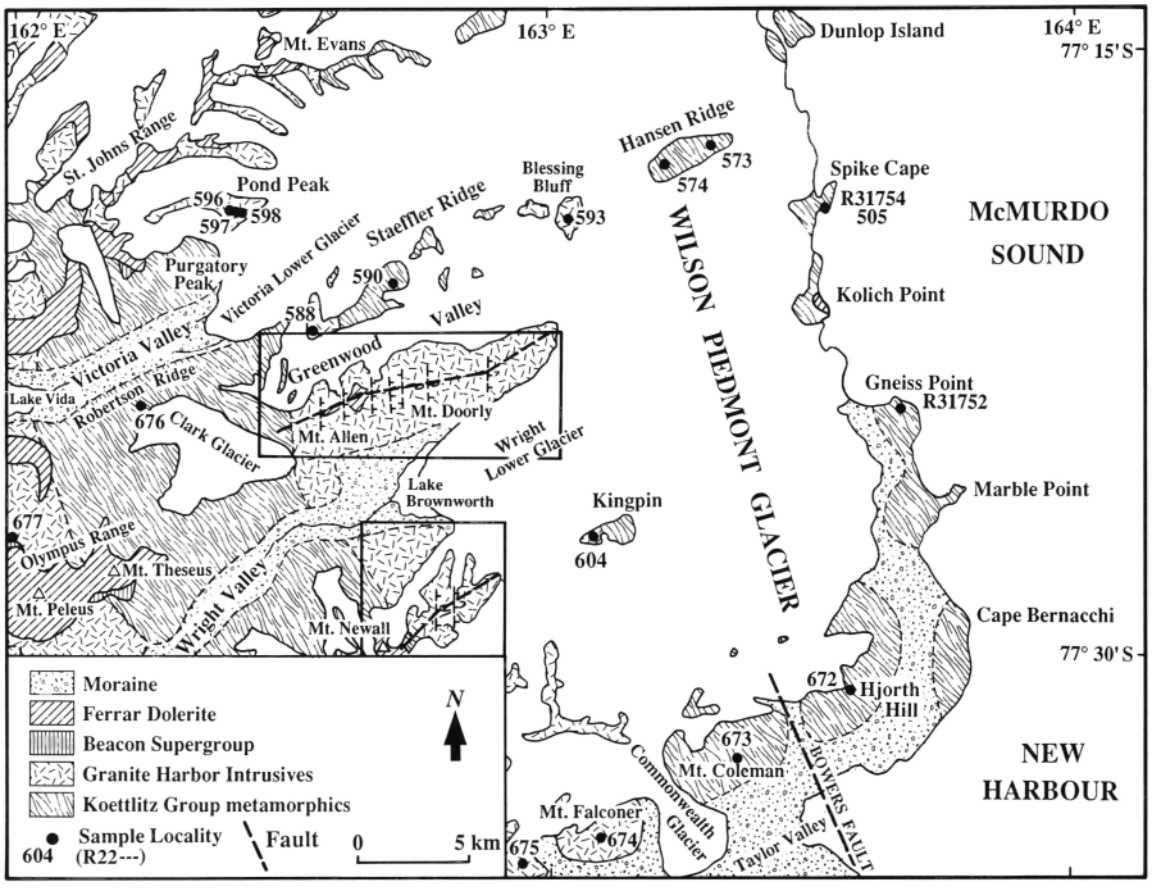

Fig. 4. Geologic map of the Wilson Piedmont Glacier area (Figure 3) showing sample localities and positions of faults (dashed lines) as determined from field evidence. Map is constructed from field observations and work of McKelvey and Webb [1962], Allen and Gibson [1962], and Lopatin [1972]. Upper boxed area over the Mount Doorly-Mount Allen ridge marks the location of Figure 5 and the line of the cross section in Figure 9. The lower boxed area over Mount Newall marks the location of Figure 6 and the line of the cross section in Figure 12.

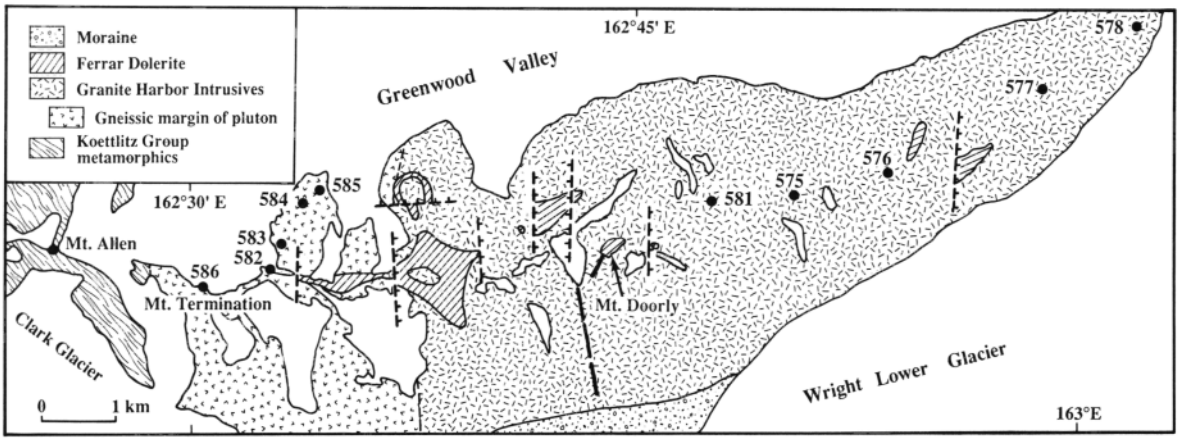

Fig. 5. Geologic map of the Mount Doorly-Mount Allen ridge system (Figure 4). The heavy dashed line to the southwest of Mount Doorly shows the position of the vertical sampling profile taken by Gleadow and Fitzgerald [1987]. Geological symbols are as for Figure 4. The gneissic margin of pluton was formerly mapped as Olympus Granite-Gneiss. Sample localities (without prefixes R22) are also shown.

The basement rocks consist of belts of metasediments that trend north-south through this region, in places intruded by granite bodies (Figure 4). The Dais Granite and Olympus Granite-Gneiss of McKelvey and Webb [1962], which crop out along the Mount Doorly spur, are now considered cogenetic, forming different phases of the same plutons [Lopatin, 1972; Skinner, 1983]. In this study, these granites are mapped simply as Granite Harbour Intrusives, as is the Vida Granite [McKelvey and Webb, 1962], that crops out further to the west in the Olympus Range. Sills of Ferrar Dolerite crop out at a number of localities, especially along the Mount Doorly spur and at Mount Newall, where the dolerite has been faulted. Dolerite caps Mount Evans and the Saint Johns Range to the north of the Victoria Lower Glacier. On the western side of the mapped area the dolerite and the Beacon sediments dip gently to the west at 2°-3°.

The Mount Doorly-Mount Allen ridge system: A primary concern in the sampling along this ridge (Figure 5) was to take samples on different sides of known faults, to test whether faulting on the order of hundreds of meters could be detected by apatite fission track analysis. If so, then the method could be applied to areas where faulting is suspected, but the magnitude is unconstrained. The dolerite sill which is offset along this ridge, and is the key to determining the structure of the TAM Front in this area, has been correlated to the basement sill of Gunn and Warren [1962] [Gleadow and Fitzgerald, 1987]. Sills of the Ferrar Dolerite in southern Victoria Land have a remarkably regular form and have been intruded along zones of horizontal weakness. The best examples are the basement sill and peneplain sill (so called because it intrudes almost perfectly along the Kukri Peneplain, between the planated granite surface and the overlying sediments of the Beacon Supergroup). In the Wright Valley, these two sills are each 250-300 m thick and parallel each other some 300 m apart. The basement sill intruded along horizontal exfoliation joints in the granitic basement beneath the peneplain [Hamilton et al., 1965] pinches out as it approaches metamorphic belts because of their irregular structure and steeply dipping nature. Dolerite is rarely seen intruding these metamorphics in the same regular manner as in the granites. Dolerite sills are also present in the sediments of the Beacon, but because of the tendency of rafts of sandstone to float on the dolerite at time of intrusion [Grapes et al., 1974], these sills tend to be narrower and less regular than in the granitic basement and are unreliable as markers of post-Jurassic faulting.

The Mount Doorly spur is composed of a grey to pale pink biotite granite, often porphyritic with laths of feldspar either randomly orientated or defining a strong north-south foliation. West of Mount Doorly, at Mount Termination, Dais Granite gives way to the Olympus Granite-Gneiss, which in turn passes into metamorphics (the Meserve Member of Findlay et al.'s [1984] Hobbs Formation of the Koettlitz Group). The basement dolerite sill along this ridge system is displaced by normal faults with a maximum throw on any one fault of ~400 m, and a cumulative displacement along the ridge system of >800 m. Granite is present above dolerite on a peak 3 km west of Mount Doorly, further evidence that this is the basement sill. Sense of offset and dip on the various segments of dolerite that display step faulting are variable. At Mount Theseus dolerite dips 3° to the west, but further to the west it flattens out to become almost horizontal. Along the Mount Allen-Mount Doorly ridge the sections of dolerite have dips of 1°-2° mainly to the west, but occasionally to the east. At the eastern end of the Mount Doorly spur, the dip of the dolerite is slightly steeper (3°-4°) to the west, possibly indicating minor rotation of the fault blocks and suggesting that the fault planes become listric at depth. The faults cutting the Mount Doorly spur are reflected in the topographic profile, in places forming small scarps suggesting continued movement up to the present day. Other evidence for faulting are north-south trending crush zones.

The strike of the individual faults is difficult to determine with great precision, but they all generally strike NNW-SSE through NNE-SSW. Preliminary results from detailed structural work along the Mount Doorly spur indicate that the dominant strike direction of the faults is NNE-SSW [T. Wilson, personal communication, 1990]. On the northern ridge of the peak 3 km to the west of Mount Doorly an east-west trending normal fault offsets a thin band of dolerite (15-20 m thick) down to the north by ~100 m. This band of dolerite is probably the thinned extremity of the dolerite sill present along the main ridge system and shows that east-west trending normal faulting may exist in a similar fashion to the approximately north-south trending faults which are so poignantly displayed by the offset dolerite sills along the Mount Doorly spur.

A fault is suspected running east-west up the Greenwood Valley (Figure 4) for a number of reasons: (1) No dolerite exists on Staeffler Ridge, this suggests that Staeffler Ridge has been upthrown relative to the Mount Doorly-Mount Allen ridge system. The lack of dolerite, however, could also be explained by the dolerite sill pinching out as it approaches metamorphic rocks, as described above. (2) The rock types on Staeffler Ridge are discordant to those seen across the Greenwood Valley on the Mount Doorly spur. On Staeffler Ridge there is no transition from Dais Granite through its foliated border phase to metamorphics. Dais Granite is present only at the far eastern end of the ridge, which is otherwise dominated by metamorphics. Gleadow et al. [1984] proposed a fault, downthrown to the north by ~400 m, between Lake Vida and the southern side of the Victoria Valley. The dolerite outcrop pattern at the western end of Lake Vida appears to double in width and possibly marks the location of this fault. Although the sense of offset for this fault differs from that suggested for the Greenwood Valley fault, it is possible the two are related.

Other localities: Hansen Ridge is a east-west trending elongate nunatak 3-4 km inland from the McMurdo Sound coast (Figure 4). It is composed dominantly of NNE striking, steeply dipping bands of biotite schist with intercalated marble, strongly foliated metadiorite, and minor quartz-feldspar-biotite schist and leucogranite veins. These lithologies are most likely part of Findlay et al.'s [1984] Marshall Formation of the Koettlitz Group. Staeffler Ridge also contains a significant proportion of metamorphics, especially toward its western end where it is dominated by biotite schist, quartzo-feldspathic gneiss, metadiorite, metagranodiorite, and amphibolite. Staeffler Ridge in places is cut by vertical dolerite dikes that strike northeast. Along its length, but especially toward the western end, a number of north-south trending scree-filled gullies indicate possible crush zones and fault traces. Looking from the south at a distance, dikes in the metamorphics of the western part of the ridge appear to be offset, downthrown to the east in two or three places, but with throws of only ~20-30 m. The ridge was sampled along its length, from the west (R22588) eastward to Blessing Bluff (R22593). Three samples of massive biotite granite were collected from the east ridge of Pond Peak.

Mount Newall, ~10 km to the south of Mount Doorly across the Wright Valley, is composed of a rock type similar to

that at Mount Doorly, a dominantly uniform pale grey to pale pink biotite granodiorite, porphyritic in places. To the west, the granodiorite gives way to metamorphics composed of augengneiss, gabbro, quartz-feldspar-biotite gneiss, amphibolite, and mica schist. Mount Newall is capped by a dolerite sill that dips gently westward. At a number of localities down the northeast ridge, dolerite caps small knolls at successively lower elevations (Figure 6) indicating faulting similar to that along the Mount Doorly spur. A total displacement of ~700 m, down to the east, is evident between the dolerite occurring along the ridge and that capping the summit of Mount Newall. The northeast ridge of Mount Newall was sampled from near the summit (R22605) to its easternmost point (R22610). A vertical sampling profile covering 330 m (R22611-R22614) was taken off the southeast spur along the ridge to complement another vertical sampling profile (samples R31745-R31748) taken off the northern slopes of Mount Newall by Gleadow and Fitzgerald [1987].

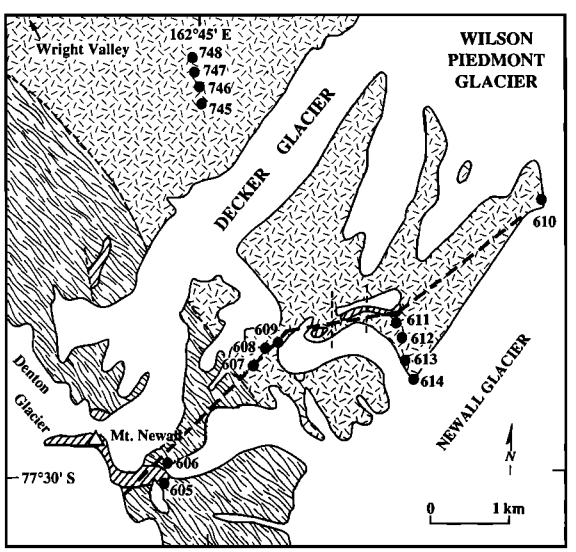

Fig. 6. Geologic map of the Mount Newall east ridge (Figure 4). Faults are shown as thin dashed lines and the heavy dashed line shows the line of the cross section shown in Figure 12. Sample localities (without prefixes R22) are also shown, as are the positions of four samples (R31745-R31748) from a vertical profile taken by Gleadow and Fitzgerald [1987] on the northern flank of the Mount Newall massif.

Kingpin (Figure 4), a small nunatak east of Mount Newall, is composed of metamorphics, amphibolite, biotite schist with saccharoidal marble bands at its eastern end, and granodiorite, extremely gneissic except at the western end (sample R22604). A horizontal sampling traverse was collected across the southern end of the Wilson Piedmont Glacier and northern side of New Harbour. Hjorth Hill (R22672), Mount Coleman (R22673), the Mount Falconer pluton (R22764), and the east ridge of Mount McLennan (R22675) were sampled. There is an obvious fault just to the east of Mount Coleman, marked by a change in slope and offset dikes. This is the Bowers fault of Gunn and Warren [1962].

Structure of the Wilson Piedmont Glacier area: The simple tilt-block structure of the TAM is clearly shown by the gentle westerly dip of the Kukri Peneplain and the dolerite sills in the Wright and Victoria valleys. The peneplain sill has a steeper dip near its most eastern extent at Mount Theseus (~5° west) before flattening out to become nearly horizontal at Mount Jason (dip of <1° west). The basement sill exhibits a similar structure, having a steep dip near Mount Theseus and Purgatory Peak, where it actually bends up toward the peneplain sill before flattening in dip to the west and maintaining a near parallel relationship with the peneplain sill. Evidence for north-south faulting across the TAM Front is seen dominantly in the form of displaced dolerite sills, evident along the Mount Doorly spur and at Mount Newall. Dolerite, identified as the basement sill, is also found near coastal levels at Kolich Point [Gleadow and Fitzgerald, 1987]. The dolerite sills define an axis, where the TAM are at their highest level structurally before entering the faulted TAM Front. The TAM Front, from field evidence alone, is typified by a zone of normal faults that have nearly vertical fault planes, although these faults may become listric at depth. In extent, the TAM Front ranges from an axis of maximum structural expression between Mount Doorly and Mount Allen to at least the McMurdo Sound coast. Over this distance, the cumulative offset is ~2 km down to the east assuming a constant westerly dip of ~2°-3° for the fault blocks across the mountain front.

The Granite Harbour Region

Granite Harbour (Figure 7) is the type locality for all plutonic and hypabyssal intrusives that invaded the sediments of the Ross System and are older than the Kukri Peneplain [Gunn and Warren, 1962]. The intrusives range in composition from granites to quartz diorites [Palmer, 1987]. Strata of the Beacon Supergroup constitute only a small portion of the mapped area and are seen as thin wedges between the peneplain dolerite sill and the granitic or metamorphic basement (e.g., at the northwest corner of Killer Ridge, the western side of the Miller Glacier opposite Queer Mountain, at Mount Suess, and in the Clare Range). Pegtop Mountain and Mount Woolnough, at the western edge of the mapped area, are composed substantially of Beacon and dolerite. Dolerite crops out mainly in the western part of the area but also caps the Kar Plateau on the north side of the harbour, one of its most easterly onland localities in the McMurdo region. Dolerite also caps spot height 1540, ~9 km southwest of Mount England, and increases in extent and thickness to the west because of its gentle westerly dip.

Granite Harbour and the polar-plateau-fed Mackay Glacier cut a cross section through the TAM, which allowed collection of a line of samples from Cape Roberts (R22507) westward along the coast and then inland up the New Glacier as far as the Clare Range (R22557). Samples were taken every few kilometers over the region where the faulted TAM Front was expected to extend, and then approximately every 5 km on the inland section. As regards sampling logistics, Granite Harbour falls naturally into three areas, the south side of the harbour, inland of the harbour on the south side, and the north side of the harbour.

The south side of Granite Harbour: A vertical sampling profile of eight samples over ~1200 m elevation was taken on the north face of Mount England (Figure 7). Two obvious faults exist on the north face to the east of the vertical profile (Figure 8), indicated by the presence of two steep, very straight, scree-filled gullies containing slickensides. One fault appears upthrown to the east because of the topographic expression shown at the top of the gully. A horizontal sampling profile was taken from Cape Roberts (R22507) to the base of the east

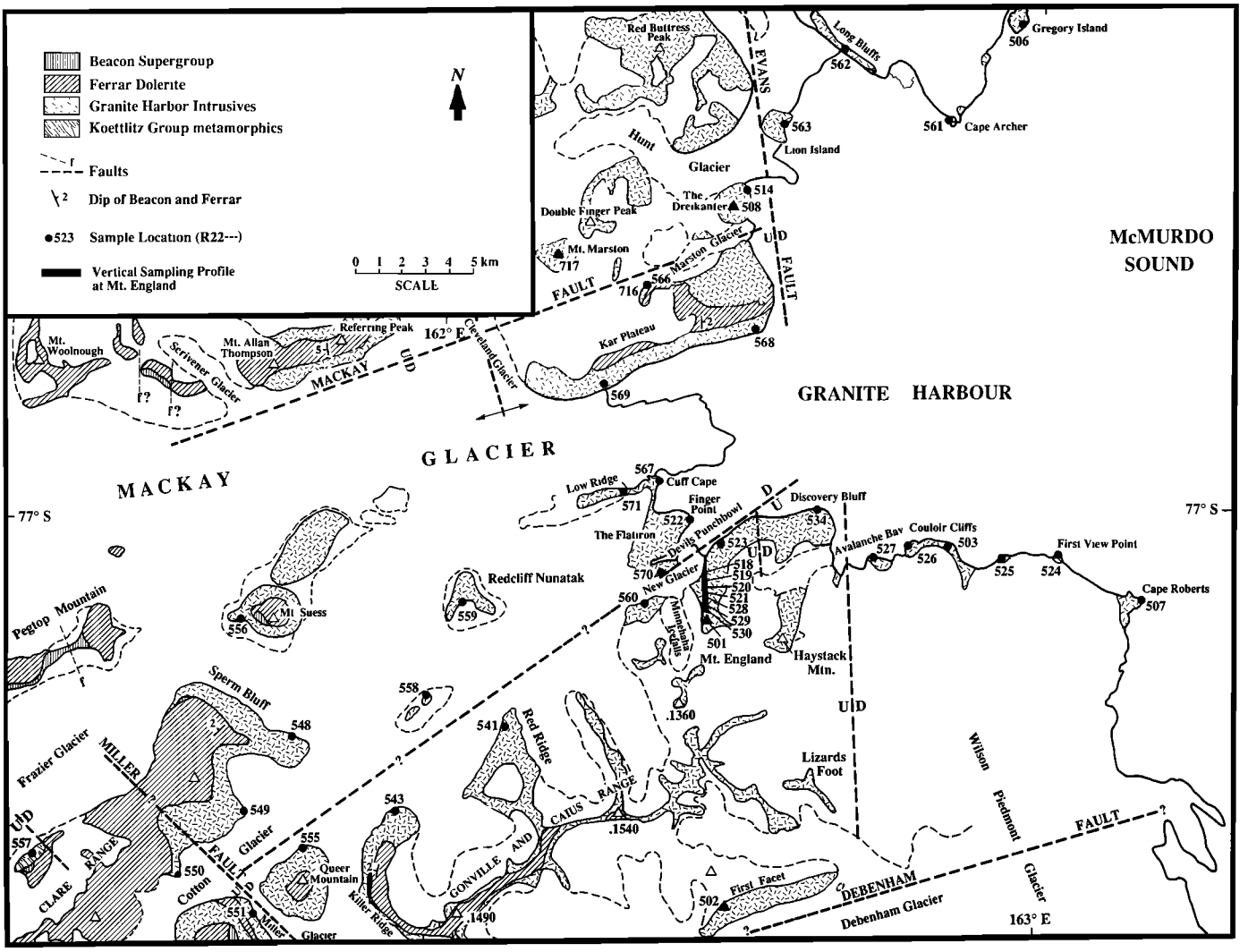

Fig. 7. Geologic map of the Granite Harbour region (Figure 3) showing geology, sample localities (without prefixes R22), and positions of faults (dashed lines) as determined from field evidence. Map is constructed from field mapping and from work of Gunn and Warren [1962].

DIAGRAMMATIC CROSS SECTION: QUEER MOUNTAIN TO CAPE ROBERTS

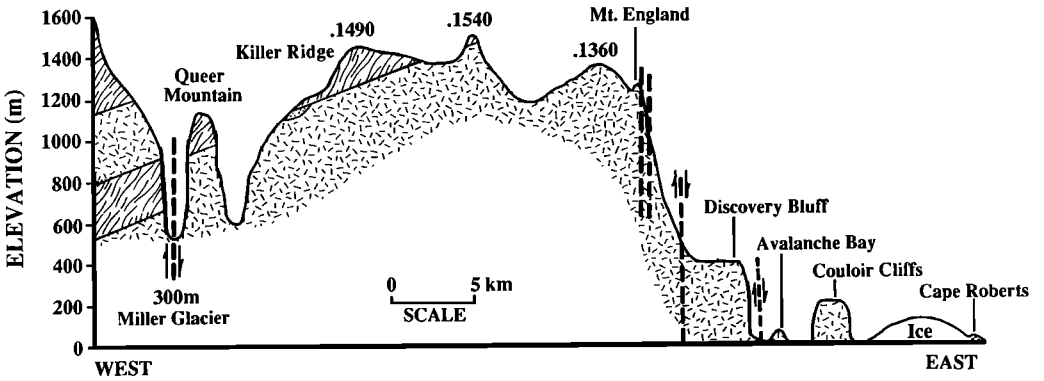

Fig. 8. Cross section from the western side of the Miller Glacier, along the crest of the Gonville and Caius Range, through Mount England, and across the southern side of Granite Harbour to Cape Roberts (Figure 7).

ridge of Mount England (R22523). The rocks on the western margin of Couloir Cliffs are jointed, with jointing becoming increasingly severe and sheared toward Avalanche Bay. This jointing is probably indicative of the edge of a small pluton, although a fault probably exists through Avalanche Bay, as suggested by Gunn and Warren [1962] from extrapolation of the possible fault scarp on the east side of Haystack Mountain and the Lizards Foot. Another abrupt topographic escarpment on the east flank of Mount England possibly marks another fault.

Inland of Granite Harbour: The horizontal sampling transect along the southern shores of Granite Harbour was continued on a northeast-southwest line inland up New Glacier and to the Cotton Glacier (Figure 7). A major fault exists between Queer Mountain and the western side of the Miller Glacier as revealed by an offset in the dolerite sills (Figure 8). A sliver of Beacon sandstone is exposed at the base of the dolerite sill on Killer Ridge indicating this is the peneplain sill. The base of this sill on Killer Ridge is at an elevation of ~1000 m and has a dip of 2°-3° to the WNW. The base of the dolerite sill at Queer Mountain is at a lower elevation (~900 m) than the sill on Killer Ridge, consistent with the shallow westerly dip of the dolerite, and is also the peneplain sill, although no sandstone is seen at Queer Mountain. Two dolerite sills are evident on the western side of the Miller Glacier, the basement sill and the peneplain sill. The base of the peneplain sill on the western side of Miller Glacier is at an elevation of ~1200 m. Taking into account the dip of the dolerite, Queer Mountain is downthrown some 300-400 m relative to the western side of the Miller Glacier. This is the Miller fault of Gunn and Warren [1962]. The Miller fault most likely extends north of the Cotton Glacier. Basement rock at sample site R22557 also appears to be faulted up into position.

Sperm Bluff is composed dominantly of adamellite with gneissic inclusions and capped by dolerite, with the base of the dolerite at its eastern end at an elevation of ~900 m. Dolerite on Sperm Bluff dips to the WNW-NNW at ~2°. A gully on its northeastern flank separates a roche moutonnee from the bulk of Sperm Bluff. This gully trends 153° in a line down the Miller Glacier and marks a possible fault. Another possible fault trace is marked by a deeply incised trench that crosses the eastern extension of Sperm Bluff and trends 188°. The presence of a large block of Beacon sandstone amongst dolerite between Mount Woolnough and Scrivener Glacier on the northern side of the MacKay Glacier indicates possible faulting.

The north side of Granite Harbour: A horizontal sampling traverse was collected from Gregory Island to the Kar Plateau (Figure 7). A vertical sampling profile of 550 m was collected from The Dreikanter. Samples were taken on either side of the Marston Glacier to see whether the ~800 m offset, down to the south, of the Mackay fault [Gunn and Warren, 1962] would be observable in the fission track results. Gunn and Warren noted that while dolerite caps the Kar Plateau (with the base of the sill at an elevation of ~200 m and dipping gently to the east), it does not reappear on the northern side of the Marston Glacier until an elevation of at least 1000 m on Mount Broger (not shown on Figure 7 but it lies ~5 km west of Red Buttress Peak). Gunn and Warren therefore proposed a fault up the Marston Glacier, with an offset of at least 800 m down to the south. No dolerite is present on Mount England to the south of the Mackay Glacier, and so it is likely that a fault exists between Mount England and the Kar Plateau. It was hoped that by sampling on a north-south line from the Kar Plateau across Cuff Cape, the Flatiron, and New Glacier the position of such a major fault between the Kar Plateau and Mount England would be revealed by the fission track results. No dolerite is present on The Flatiron, but this is a low-relief feature, and the absence of dolerite may simply reflect this low relief.

The dolerite on Referring Peak dips to the west at ~5° and is capped by Beacon strata further to the west, indicating that it is the peneplain sill. In contrast, dolerite on the Kar Plateau dips gently east, indicating that a hinge line exists between the two areas, striking approximately north-south up the Cleveland Glacier.

Structure of the Granite Harbour area: Evidence for faulting is from displaced dolerite sills, NNW trending crush zones, and fault traces within the granite bodies. On the south side of Granite Harbour a number of faults are evident (Figure 7). A fault between Mount England and Avalanche Bay is also suspected on geomorphological grounds because of the marked reduction in summit elevations to the east [Gunn and Warren, 1962]. The fault up the Miller Glacier is defined by the offset of the peneplain sill, and because it offsets the dolerite, it is post-Jurassic in age. However, faults defined by dolerite sills within the Beacon strata (e.g., at Pegtop and Mount Woolnough) are probably contemporaneous with dolerite intrusion, as discussed above.

The faults discussed above all have a general NNW-SSE trend. The Mackay fault of Gunn and Warren [1962] has an northeast-southwest trend up the Marston Glacier and has a throw of at least 800 m, down to the south. The absence of dolerite on Mount England implies that another fault (most likely up New Glacier) of similar magnitude but opposite sense of displacement must be present between the Kar Plateau and Mount England; this suggests that the Mackay Glacier exits to McMurdo Sound through a graben. Gunn and Warren [1962] also proposed a fault up the Debenham Glacier on the basis of discordant rock types across the glacier and the magnificent scarps displayed by the First and Second Facets on the north side of the Debenham Glacier. From field evidence alone it is not known whether the hinge line up the Cleveland Glacier extends south across the Mackay Glacier. Apart from the easterly dip of the dolerite on the Kar Plateau, all dolerite in this area dips to the west or west-northwest at angles of 2°-5°. Therefore the structure of the mountains in this area would seem to be a series of fault blocks, in general tilted gently to the west.

RESULTS

Sample elevations were measured barometrically as described by Gleadow et al. [1984]. Apatites were separated from the host rock using standard magnetic and heavy liquid techniques and dated using the external detector method [Moore et al., 1986] with an Autoscan™ stage. Samples were irradiated in the X-7 position of the Australian Energy Commission HIFAR Research Reactor, which has a well-thermalized flux (Cd ratio for Au activation ~125). Thermal neutron fluences were monitored by recording the track density in a muscovite detector attached to discs of the U.S. National Bureau of Standards reference glass SRM612. The mounts were counted at a magnification of 1250X under a 80X dry objective at the University of Melbourne, and ages were determined using the zeta method of calibration, following the procedures of Hurford and Green [1983] and Green [1985]. Errors were calculated using the conventional method [Green, 1981] and are quoted in the text at a level of $\pm 1\sigma$ but are presented in diagrams at $\pm 2\sigma$.

Horizontal confined track lengths were measured at Arizona State University, Tempe, at a magnification of 1250X under a 100X dry objective using a drawing tube and a digitizing tablet, based upon the methods, recognition criteria, and identification procedure of Laslett et al. [1982, 1984] and Gleadow et al. [1986a, b].

The Wilson Piedmont Glacier Area

The Mount Doorly-Mount Allen ridge system: Apatites range in age (Table 2) from 63 ±7 Ma at the eastern end to 95 ±4 Ma at Mount Allen (Figure 9). Ages, in general, are very similar and many lie within error limits of each other. However, sample elevations decrease to the east, and, as will be shown below, this is evidence of faulting with displacements consistent with those determined from offset dolerite sills. The Mount Doorly profile [Gleadow and Fitzgerald, 1987] may actually cross two small faults (Figure 9). However, this does not affect the interpretation because the magnitude of each fault is small and they have different senses of movement, effectively cancelling any noticeable effect in the age-elevation profile. Track length distributions (e.g., sample R22576, Figure 10) have mean lengths ≤13.8 μm with standard deviations ≥1.7 μm, similar to distributions reported by Gleadow and Fitzgerald [1987] for ages >50 Ma on the Mount Doorly profile. Sample R22677 from the Olympus Range has an age of 155 ±9 Ma. It has a mean length of 12.7 μm with a standard deviation of 2 μm, similar to distributions for similar ages obtained from the Mount Jason vertical profile [Gleadow and Fitzgerald, 1987].

Other localities: Samples from Hansen Ridge yielded ages (Table 2 and Figure 11) of 69 ±3 Ma (eastern end) and 91 ±4 Ma (western end). Ages from Staeffler Ridge range from 73 ±5 Ma (middle of ridge) to 83 ±9 Ma (Blessing Bluff) and are similar to ages from along the Mount Doorly spur at similar elevations and at similar relative positions within the mountain front. Ages from Pond Peak vary from 95 ±5 Ma (1300 m) to 88 ±7 Ma for the lowermost of the three samples (1100 m), although the difference is not statistically significant. Track length distributions (e.g., samples R22588 and R22605, Figure 10) for all samples measured from these localities (Table 2) are very similar to those from along the Mount Doorly ridge system east of Mount Allen.

Ages from Mount Newall range from 130 ±16 Ma (near summit) to 64 ±6 Ma (end of the northeast ridge) (Table 2 and Figure 12). The four samples across the southern end of the piedmont glacier have ages from 66 ±5 Ma to 73 ±5 Ma (Figure 11). Track length distributions for these four samples (e.g., sample R22675, Figure 10) are similar to those from samples along the Mount Doorly ridge system east of Mount Allen.

Granite Harbour

The south side of Granite Harbour: Ages from Mount England (Table 3) range from 96 ±4 Ma (summit) to 51 ±6 Ma (lowermost sample at the base of the north face). Ages decrease uniformly with elevation (Figures 13 and 14) defining a shallow gradient of ~15 m/m.y. down to an elevation of ~500 m, below which ages remain essentially constant, defining a much steeper gradient. Track length distributions (Table 3 and Figure 14) from samples above this break in slope at 500 m and ~55 Ma have mean lengths ≤13.4 μm and standard deviations ≥2 μm. Length distributions for these samples are generally broad and sometimes bimodal. Samples below the break in slope have mean lengths ≥14.0 μm and standard deviations ≤1.6 μm. These distributions are narrower and have a smaller short track component than distributions above the break, although there are still short tracks present.

Ages along the southern coast (Figure 13) show a general increase eastward, from 43 ±3 Ma at the base of the east ridge of Mount England to 88 ±9 Ma at Cape Roberts. Ages from the Devils Punchbowl-Cuff Cape area (between New Glacier and the Mackay Glacier) range from 45 ±4 Ma to 62 ±8 Ma. Track length distributions (Table 3) for samples <56 Ma (e.g., samples R22522 and R22534, Figure 15) have means ≥14.0 μm with standard deviations ≤2.0 μm, whereas the two length distributions for samples >56 Ma have means ≤13.5 μm and standard deviations ≥2.0 μm (e.g., sample R22507, Figure 15).

Inland of Granite Harbour: Just west of Minnehaha Icefall on the western flank of Mount England the youngest apatite age (31 ±2 Ma) in the Granite Harbour area was obtained. Continuing inland the ages progressively increase, from 92 ±3 Ma at Red Ridge to 103 ±6 Ma at Queer Mountain (Figure 13). The age on the west side of the Miller Glacier (R22551) is 46 ±3 Ma, consistent with the sense of displacement (up to the west) determined from the offset dolerite sills. The sense of offset can be determined because apatite ages vary with elevation, younger ages residing at lower elevations (Figures 2 and 14), and hence younger ages indicate the upthrown side. This principle of determining the sense and magnitude of displacement across normal faults using offset apatite age is used frequently throughout this paper and is developed more thoroughly below. Length distributions for samples from this area (Table 3) follow the same trend seen at Mount England and along the south coast of Granite Harbour, where ages <56 Ma have relatively long mean lengths and a narrow distribution, whereas ages >56 Ma (e.g., sample R22555, Figure 15) have a somewhat shorter mean length and a broader distribution. The western most sample (Clare Range) has the oldest age of 172 ±10 Ma, which only just postdates the time of intrusion of the Ferrar Dolerite (179 ±7 Ma [Kyle et al., 1981]). This sample (R22557, Figure 15) also has a significantly shorter mean length (12.5 μm) compared to other samples with ages >56 Ma in this area.

The north side of Granite Harbour: Along the northern shores (Figure 13), ages vary little and range from 44 ±6 Ma at Long Bluffs to 61 ±6 Ma at Gregory Island. The top and bottom samples from The Dreikanter show no significant variation of age with elevation, similar to the lack of variation in age seen in the lowermost samples of the Mount England profile (Figure 14). Samples at low elevations from either side of the MacKay fault do not show any variation in age, such as across the Miller fault. Indeed, apart from the sample from the top of Mount Marston (87 ±4 Ma), all of the ages from this area are very similar. Length distributions (Table 3) follow the same trend seen in all other areas: ages <56 Ma have relatively long mean lengths and a narrow distribution (e.g., sample R22716, Figure 15), whereas ages >56 Ma have a somewhat shorter mean length and a broader distribution.

DISCUSSION

Timing of Uplift

The application of apatite fission track analysis to studies of uplift and denudation of mountain belts is discussed in detail by Fitzgerald and Gleadow [1988, 1990]. As found in previous fission track studies of the TAM in southern Victoria Land

TABLE 2. Apatite Fission Track Analytical Results: Wilson Piedmont Glacier Area

Sample	Locality	Elevation, m	Number of Grains	Standard Track Density ($\times10^6$ cm^{-2})	Fossil Track Density ($\times10^6$ cm^{-2})	Induced Track Density ($\times10^6$ cm^{-2})	Correlation Coefficient	Chi Square Probability %	Age Ma	Uranium ppm	Mean Track Length µm	Standard Deviation µm
				Mount Doorly-Mount Allen Ridge System Westward to the Olympus Range								
R22575	Mount Doorly eastern spur (spot height 884)	884	24	4.08 (3575)	0.529 (172)	3.877 (1260)	0.859	7	98 ± 8	12	13.8 ± 0.20 (100)	2.0
R22576	Mount Doorly eastern spur	846	21	3.44 (6022)	0.351 (162)	2.509 (1158)	0.811	17	85 ± 7	10	13.4 ± 0.26 (79)	2.3
R22577	Mount Doorly eastern spur	753	19	3.44 (6022)	0.335 (112)	2.357 (787)	0.940	97	86 ± 9	9		
R22578	Mount Doorly eastern spur	561	20	3.44 (6022)	0.322 (91)	3.102 (876)	0.887	55	63 ± 7	12		
R22581	Mount Doorly eastern spur	1063	20	3.44 (6022)	0.842 (391)	6.073 (2819)	0.994	44	84 ± 5	24		
R22582	peak 4.5 km west of Mount Doorly	1400	18	1.37 (7701)	2.386 (1296)	5.875 (3191)	0.967	7	98 ± 3	56	13.8 ± 0.19 (100)	1.9
R22583	peak 4.5 km west of Mount Doorly	1305	11	1.36 (11851)	3.463 (1165)	8.914 (2999)	0.992	44	93 ± 3	86		
R22584	peak 4.5 km west of Mount Doorly	1204	12	1.36 (11851)	3.043 (1085)	8.935 (3186)	0.967	6	82 ± 3	87	13.6 ± 0.17 (100)	1.7
R22585	peak 4.5 km west of Mount Doorly	1113	20	1.15 (2193)	2.560 (1083)	6.544 (2768)	0.840	4	79 ± 3 83 ± 6*	75		
R22586	Mount Termination, 5.5 km west of Mount Doorly	1518	20	1.38 (10135)	2.173 (832)	6.302 (2413)	0.904	<1	84 ± 4 82 ± 5*	60	13.3 ± 0.18 (100)	1.8
R22587	Mount Allen	1406	20	1.38 (10135)	1.752 (677)	4.462 (1724)	0.922	39	95 ± 4	44	13.3 ± 0.18 (100)	1.8
R22676	Robertson Ridge	980	20	1.59 (3609)	2.528 (679)	9.179 (2465)	0.972	24	77 ± 4	76		
R22677	Olympus Range	1675	16	1.25 (2188)	3.303 (618)	4.656 (871)	0.950	58	155 ± 9	4	12.7 ± 0.20 (100)	2.0
				Pond Peak (Victoria Lower Glacier)								
R22596	Pond Peak, summit	1300	20	3.44 (6022)	1.059 (407)	6.746 (2593)	0.982	10	95 ± 5	2	13.6 ± 0.21 (72)	1.8
R22597	Pond Peak, east ridge	1200	20	3.44 (6022)	0.524 (141)	3.593 (967)	0.952	45	88 ± 8	14		
R22598	Pond Peak, east ridge	1100	20	3.44 (6022)	0.547 (196)	3.756 (1347)	0.976	75	88 ± 7	15		
				Hansen and Staeffler Ridges								
R22573	Hansen Ridge, east end	514	20	1.38 (10135)	1.225 (816)	4.331 (2885)	0.952	15	69 ± 3	4		
R22574	Hansen Ridge, west end	654	20	1.38 (10135)	1.541 (749)	4.119 (2002)	0.954	73	91 ± 4	39		
R22588	Staeffler Ridge, west end	1011	20	1.38 (10135)	2.926 (1302)	8.452 (3761)	0.950	34	84 ± 3	80	13.0 ± 0.18 (100)	1.9
R22590	Staeffler Ridge, middle	1113	12	1.60 (3490)	1.508 (261)	5.806 (1005)	0.985	90	73 ± 5	48		
R22593	east end of Staeffler Ridge (Blessing Bluff)	769	20	3.44 (6022)	0.272 (96)	1.986 (701)	0.782	71	83 ± 9	8		
				Mount Newall Eastern Ridge System								
R22605	Mount Newall, near summit	1820	20	2.84 (4974)	0.808 (293)	3.514 (1274)	0.826	<<1	115 ± 8 130 ± 16*	16	13.2 ± 0.18 (95)	1.8
R22606	Mount Newall, east ridge	1670	15	2.84 (4974)	2.838 (1037)	18.06 (6598)	0.943	<<1	79 ± 3 78 ± 6*	83	13.2 ± 0.18 (100)	1.8
R22607	Mount Newall, east ridge	1400	20	2.84 (4974)	0.642 (187)	2.741 (798)	0.975	89	117 ± 10	12	13.1 ± 0.21 (100)	2.1
R22608	Mount Newall, east ridge	1295	20	2.84 (4974)	0.663 (186)	3.300 (926)	0.970	95	100 ± 8	16		
R22609	Mount Newall, east ridge	1185	20	2.84 (4974)	0.511 (115)	3.277 (737)	0.950	27	78 ± 8	16		
R22610	Mount Newall, base of east ridge	580	20	2.84 (4974)	0.408 (122)	3.193 (954)	0.896	48	64 ± 6	15	13.9 ± 0.17 (100)	1.7
R22611	Southeast spur off east ridge	961	21	2.84 (4974)	0.514 (116)	2.696 (608)	0.843	61	95 ± 10	12	13.1 ± 0.18 (103)	1.8
R22612	Southeast spur off east ridge	861	20	2.84 (4974)	0.417 (139)	2.342 (780)	0.790	24	89 ± 8	11	13.6 ± 0.21 (100)	2.1
R22613	Southeast spur off east ridge	737	20	2.84 (4974)	0.461 (178)	2.971 (1148)	0.977	59	78 ± 6	14	13.6 ± 0.18 (100)	1.8
R22614	Southeast spur off east ridge	629	21	2.84 (4974)	0.466 (156)	3.357 (1125)	0.987	88	69 ± 6	16	13.2 ± 0.24 (100)	2.4
R22604	Kingpin	735	21	1.62 (3542)	1.692 (997)	5.845 (3444)	0.972	<<1	83 ± 3 93 ± 6*	47	13.1 ± 0.20 (100)	2.0
				North Side of New Harbour, Samples From East to West								
R22672	Hjorth Hill	780	20	1.90 (4151)	0.846 (614)	4.297 (3118)	0.917	1	66 ± 3 73 ± 5*	30	13.4 ± 0.19 (100)	1.9
R22673	Mount Coleman	860	20	1.90 (4151)	1.274 (840)	6.942 (4576)	0.921	<<1	61 ± 3 66 ± 5*	48	13.7 ± 0.22 (108)	2.3
R22674	Mount Falconer	830	20	1.90 (4151)	0.717 (713)	3.272 (3252)	0.972	48	73 ± 3	23	13.5 ± 0.21 (100)	2.1
R22675	Mount McLennan	1300	20	1.90 (4151)	0.497 (241)	2.288 (1110)	0.897	86	73 ± 5	16	13.5 ± 0.19 (100)	1.9

Values in parentheses are number of tracks counted. Standard and induced track densities measured on mica external detectors (g=0.5), and fossil track densities on internal mineral surfaces. Ages calculated using ζ=354 for dosimeter glass SRM612 [Hurford and Green, 1983]. Errors are given as ± one standard deviation. * Mean age, used where pooled data fail χ^2 test at 5%.

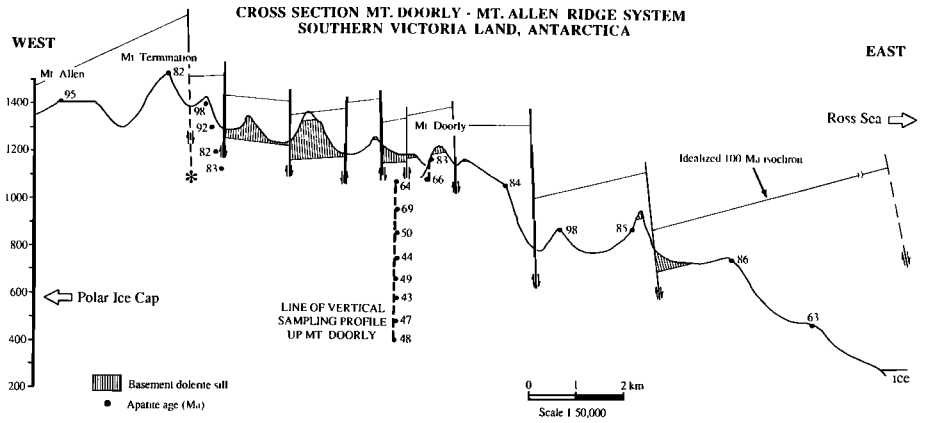

Fig. 9. Cross section through the Mount Doorly-Mount Allen ridge system, showing the offset dolerite sills and an idealized 100-Ma isochron (apatite ages) delineating the structure of the TAM Front. Although more detail is given by the dolerite sills, the overall structure can be determined by the variation of apatite ages. The asterisk marks the position of a fault determined solely from the offset in apparent ages. The line of this cross section is shown in Figure 4.

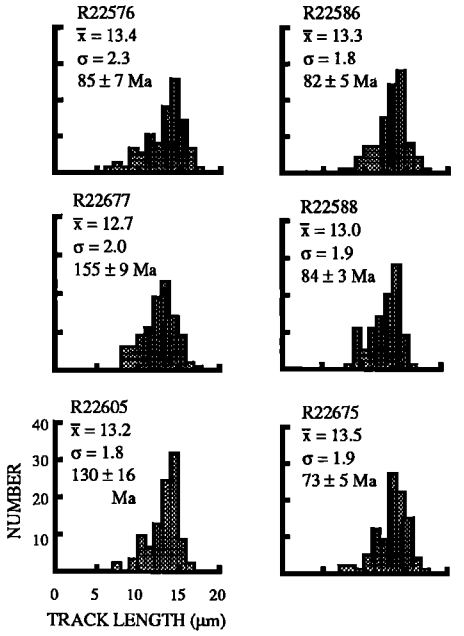

Fig. 10. Length distributions for a number of representative samples from the Wilson Piedmont Glacier area (Table 2).

[Gleadow et al., 1984; Gleadow and Fitzgerald, 1987], all apatite ages are <175 Ma. As such, they indicate a cooling history which entirely postdates the major heating accompanying emplacement of the Jurassic Ferrar Dolerite and extrusion of the Kirkpatrick Basalt (~180 Ma). Fission tracks appear to have been entirely erased from the apatites during heating accompanying magmatism, and the present pattern of ages represents a new thermal regime, most likely established during Cretaceous times.

Ages from the Mount England profile (Figure 14) have the same distinctive pattern of age versus elevation as previously noted from Mount Doorly [Gleadow and Fitzgerald, 1987]. These profiles are made up of two parts, separated by a break in slope. Above the break, ages vary significantly with elevation, defining a shallow gradient of ~15 m/m.y. Below the break, ages vary little with elevation, defining a much steeper gradient. As concluded previously [Gleadow and Fitzgerald, 1987], the break in slope in the apatite age - elevation profile represents the base of an uplifted partial annealing zone (PAZ) and is interpreted as the start of denudation following the onset of significant uplift. The age of this break is ~55 Ma at Mount England, slightly different to Mount Doorly, where it is closer to ~50 Ma. This slight variation may in part be statistical, but more likely reflects the slightly differing tectonic histories of each area or fault block. Furthermore, the presence of an uplifted PAZ means that prior to uplift there must have been a considerable period of thermal and tectonic stability following establishment of a new thermal regime after the heating accompanying Jurassic magmatism.

Apatites in samples on the steep part of the profile had apparent fission track ages of zero prior to the onset of uplift because they resided at temperatures too high to retain tracks. Apatites below the break in slope therefore did not start to retain fission tracks until cooling accompanying the uplift and associated denudation. Ideally, samples below the break have only a single component of tracks following the onset of uplift, whereas those samples above the break have a mixed component, with a contribution of tracks from the preuplift PAZ as well as a later set from the uplift phase. The break in slope of the measured apatite ages (e.g., Figure 14) is an underestimate of the actual initiation time of uplift because upon commencement of uplift, samples that define the break are annealed to a certain degree during uplift through the zone of accelerated annealing at the base of the PAZ [Wagner et al., 1989; Fitzgerald and Gleadow, 1990]. In general, if the onset of denudation that follows uplift is rapid, then the underestimate will be small. In any case, the break in slope defines a younger limit to the onset of uplift and erosion. Using forward modelling programs [Laslett et al., 1987; Green et al., 1989] to replicate the pattern of apatite ages that define the break in slope, the true initiation time of uplift is ~5 Ma prior to that seen in these profiles. Therefore the break in slope at Mount England at ~55 Ma reflects a start to uplift and denudation at ~60 Ma, and for Mount Doorly, the break at ~50 Ma reflects a start at ~55 Ma.

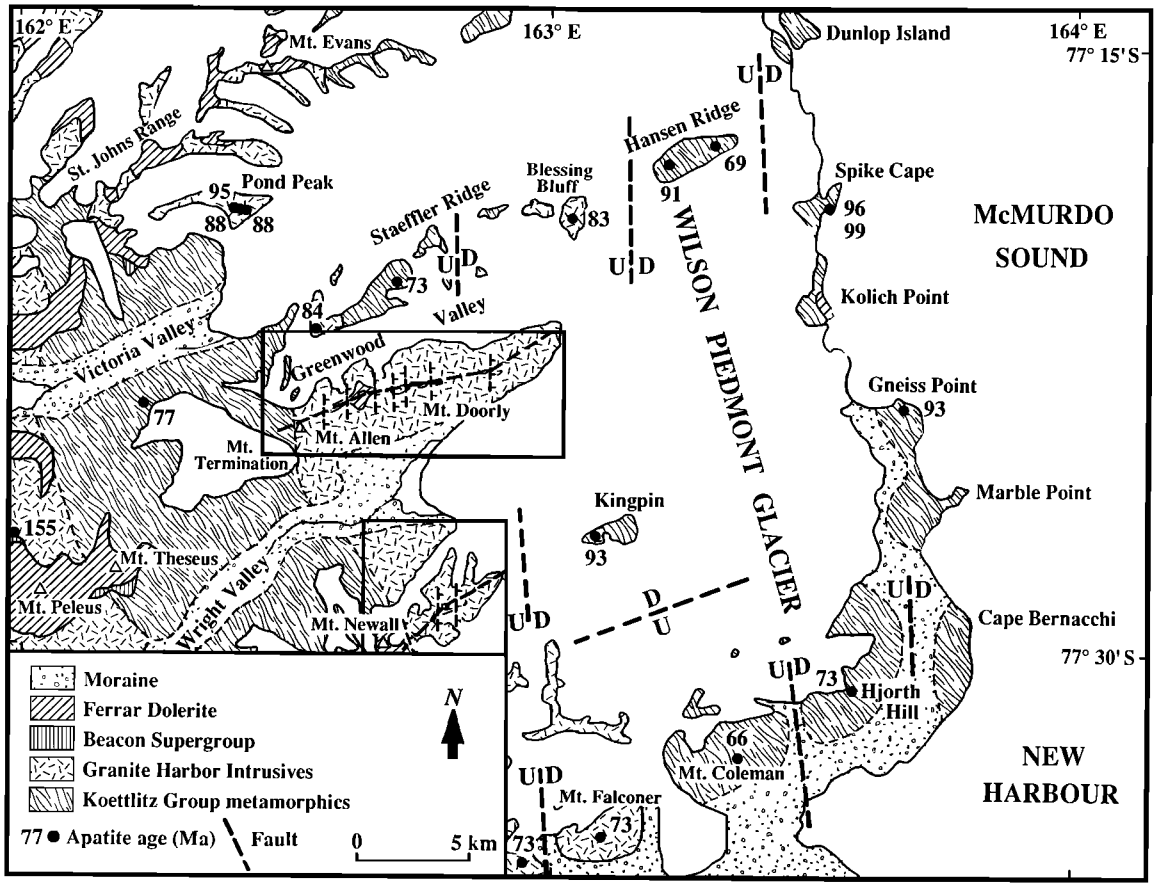

Fig. 11. Geologic map of the Wilson Piedmont Glacier showing apatite ages and faults (dashed lines) determined from field evidence and the variation of ages. Upper boxed area over the Mount Doorly-Mount Allen ridge marks the location of Figure 5 and the line of the cross section with apatite ages in Figure 9. The lower boxed area over Mount Newall marks the location of Figure 6 and the line of the cross section with apatite ages in Figure 12.

Confirmation of the interpretation of the age profile as an uplifted PAZ is given by confined track length distributions. A clear difference exists in the track length distributions for samples above and below the break in slope (Figure 14). Distributions above the break have significantly shorter mean lengths (generally <13.5 μm) and much broader distributions (standard deviations generally ≥2.0 μm) which can be bimodal. Distributions from below the break have significantly longer mean lengths (generally >13.9 μm) with correspondingly smaller standard deviations (generally <2 μm). These longer mean lengths are similar to those considered to be characteristic of undisturbed surficial volcanic rocks [Gleadow et al., 1986b], although with somewhat larger standard deviations (1.2-2.0 μm), suggesting rapid cooling from temperatures higher than the track stability range for apatite with only a relatively short residence time within the PAZ. In contrast, distributions from above the break include many short tracks, which must have undergone extensive shortening through prolonged exposure to temperatures within the PAZ.

Amount of Uplift

The amount of uplift and denudation at Mount Doorly in the lower Wright Valley was calculated by reconstructing the stratigraphy above the break in slope prior to the uplift of the TAM [Gleadow and Fitzgerald, 1987]. A total uplift of between 4.8 and 5.8 km since ~55 Ma was calculated at this locality. The same calculation would be difficult at Mount England; it is not possible to constrain the position of the break in slope with respect to the stratigraphic level because there is no dolerite at Mount England. However, the amount of uplift and denudation at Mount England can be calculated because of the similarity of apatite ages near the basement dolerite sill throughout the Dry Valleys area [Fitzgerald, 1987]. Assuming the geothermal gradient was similar throughout the area at that time, this similarity of age suggests that this sill was at the same crustal level throughout the area when the ages were set. Hence the base of the PAZ, as marked by the break in slope, was also likely to be at similar crustal levels. The amount of uplift at Mount England is therefore ~300 m less than at Mount Doorly because the elevation of the break in slope at each is at ~500 m and ~800 m, respectively.

Mount England, like Mount Doorly, lies within the confines of the faulted TAM Front, and therefore the amount of uplift and denudation at these two localities is an underestimate of the amount that has occurred along the axis of maximum uplift (the structural high) that lies inland of these two peaks. As will be discussed below, and is shown in Figure 9, the axis of

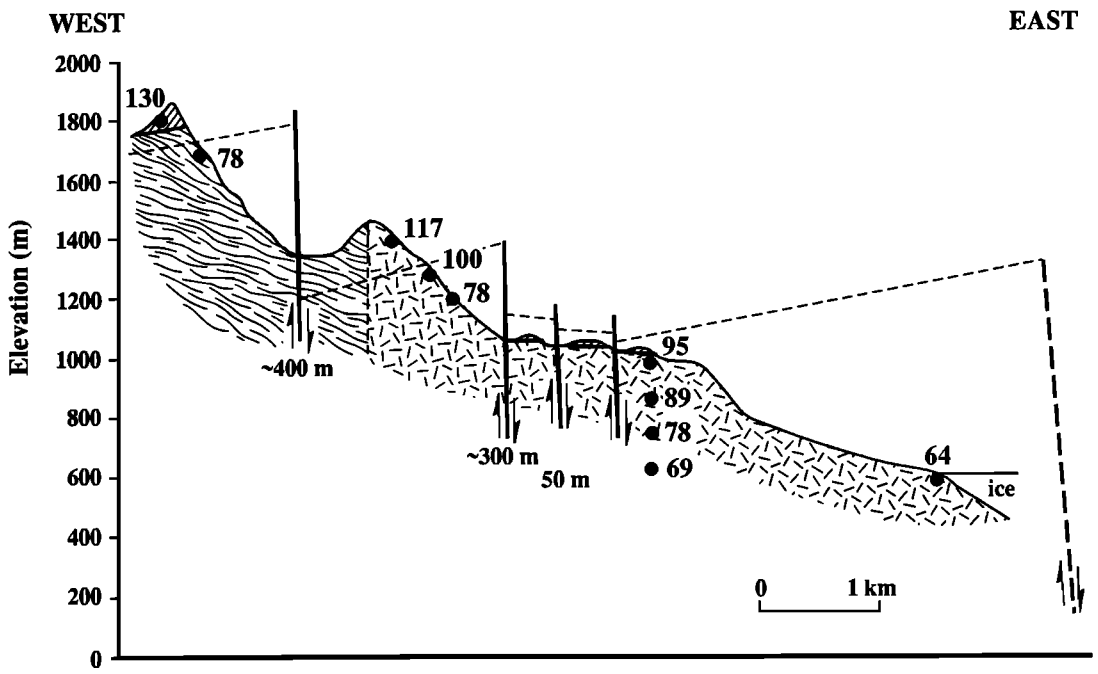

Fig. 12. Cross section through the northeastern ridge of Mount Newall (Figures 4 and 6) showing apatite ages and positions of, plus displacements across, faults inferred from these results. Ages from the vertical profile off the southern spur of the northeast ridge (R22611-R22614, Figure 6) have been projected onto the line of the cross section. Also shown on the right of the diagram is a fault (heavy dashed line) between the base of this ridge and Kingpin. The structure down the ridge is delineated by an idealized ~100-Ma isochron (thin dashed line). Map symbols are as for Figure 11.

maximum uplift inland from Mount Doorly is at Mount Termination, ~6 km west of Mount Doorly. If the displacements of the offset dolerite sills along the ridge are added, it can be seen that uplift there is ~1 km greater than at Mount Doorly or ~6.3 km since ~55 Ma.

Metamorphic grade of the lithologies present within the mapped area do not constrain the depth of burial before uplift of the TAM started in the early Cenozoic. Basement metamorphic rocks range from low to high grade and reflect a pre-Mesozoic history [Skinner, 1983; Findlay et al., 1984]. Strata of the Beacon Supergroup were overprinted by heat accompanying intrusion of the Ferrar Dolerite and extrusion of the Kirkpatrick Basalt [Haskell, 1964]. However, the fact that dolerite was intruded hypabyssally and that basalt was erupted is consistent with the amount of uplift and levels of erosion calculated in this paper.

Amount of Erosion

The amount of erosion that has occurred at some of these localities can be estimated using the fission track data. At Mount Doorly there has been ~5.3 km of uplift and at Mount England only slightly less. The elevation of the break in slope at each of these localities is 500-800 m, and the peaks themselves are at elevations of 1000-1200 m. If preuplift surface elevation was between 0 and 500 m above sea level (as estimated by Fitzgerald [1987]), then some 4-4.5 km of erosion has occurred at each of these localities. At Mount Termination (1518 m), where uplift is about 6 km, the amount of erosion can be constrained as ~4.5-5 km, assuming a preuplift surface elevation of 0-500 m. The amount of uplift, as indicated by the decreasing dip of the Kukri Peneplain and by the fission track profiles to the west [Gleadow et al., 1984], decreases markedly inland once past the axis of maximum uplift. As the elevation of the peneplain decreases, the summit elevation of the TAM progressively increases to the west, as does the completeness of the stratigraphic record. Therefore the amount of erosion decreases to the west at a greater rate than the amount of uplift. At the western margin of the TAM in the Dry Valleys, the mountains reach elevations of >2700 m (e.g., Shapeless Mountain, 2739 m), the total uplift is estimated to be 3-4 km, and so the amount of erosion is minimal compared to that further toward the coast. At the coast there has been slightly less erosion than at the axis of maximum uplift. This is seen from a comparsion of apatite ages at the coast (~96 Ma) to the slightly younger ages along the Mount Doorly-Mount Allen ridge system (~80-90 Ma), which indicate a slightly deeper crustal level and hence more erosion along this ridge. The present low elevation of the coastal outcrops is a result of faulting across the TAM Front. Within the TAM Front, faulting at shallow levels after uplift (i.e., post-early Cenozoic) best explains the pattern of apatite ages.

Paleogeothermal Gradient

Gleadow and Fitzgerald [1987] estimated a late Cretaceous paleogeothermal gradient of some 25-30°C/km based on the

TABLE 3. Apatite Fission Track Analytical Results: Granite Harbour Region

Sample	Locality	Elevation m	Number of Grains	Standard Track Density ($x10^6 cm^{-2}$)	Fossil Track Density ($x10^6 cm^{-2}$)	Induced Track Density ($x10^6 cm^{-2}$)	Correlation Coefficient	Chi Square Probability %	Age Ma	Uranium ppm	Mean Track Length µm	Standard Deviation µm
					Mount England Vertical Profile							
R22518	rib to left of central couloir, north face	76	26	3.365 (23556)	0.263 (89)	3.037 (1027)	0.987	90	51 ± 6	12	14.0 ± 0.24 (49)	1.6
R22519	rib to left of central couloir, north face	222	24	1.46 (12801)	0.271 (117)	1.197 (517)	0.983	84	58 ± 6	11	14.1 ± 0.23 (69)	1.9
R22520	rib to left of central couloir, north face	358	20	1.46 (12801)	0.510 (207)	2.290 (931)	0.990	98	57 ± 4	21	14.0 ± 0.20 (79)	1.8
R22521	rib to left of central couloir, north face	477	19	1.46 (12801)	0.236 (145)	1.176 (723)	0.981	98	51 ± 5	11	14.0 ± 0.16 (100)	1.6
R22528	central couloir, north face	610	26	1.46 (12801)	0.310 (233)	1.310 (985)	0.968	84	61 ± 4	12	13.4 ± 0.21 (94)	2.0
R22529	central couloir, north face	792	21	1.46 (12801)	0.340 (136)	1.239 (495)	0.915	53	70 ± 7	12	13.3 ± 0.23 (91)	2.2
R22530	central couloir, north face	985	25	1.31 (9539)	0.779 (496)	2.173 (1384)	0.909	87	82 ± 4	22	13.0 ± 0.21 (104)	2.2
R22501	summit	1205	17	1.46 (12801)	2.074 (885)	5.534 (2361)	0.946	50	96 ± 4	50	12.9 ± 0.21 (102)	2.1
				South of Mackay Glacier (Granite Harbour Area)								
R22502a	First Facet	~1100	19	1.46 (12801)	1.076 (801)	3.321 (2472)	0.943	59	83 ± 3	30	13.1 ± 0.20 (100)	2.0
R22502b	First Facet		15	1.46 (12801)	1.505 (816)	4.531 (2457)	0.886	15	85 ± 4	30		
R22503	Couloir Cliffs trig point	148	26	1.46 (12801)	0.342 (146)	1.181 (438)	0.896	80	85 ± 8	8		
R22507	Cape Roberts	7	20	1.46 (12801)	0.903 (493)	2.632 (1607)	0.813	<<1	78 ± 4 88 ± 9*	24	13.5 ± 0.22 (100)	2.2
R22522	The Flatiron, Finger Point	5	21	1.36 (11790)	0.725 (298)	3.456 (1420)	0.872	27	50 ± 3	34	14.3 ± 0.14 (100)	1.4
R22523	Mount England, base of east ridge	25	20	1.46 (12801)	0.676 (368)	4.005 (2179)	0.957	18	43 ± 3	36	14.0 ± 0.20 (100)	2.0
R22524	First View Point	5	23	1.46 (12801)	0.603 (576)	1.194 (1829)	0.940	3	80 ± 4 83 ± 6*	18		
R22525	Couloir Bay, east side	1	25	1.46 (12801)	0.342 (165)	1.181 (570)	0.896	31	74 ± 7	11		
R22526	Couloir Cliffs, western end	3	24	1.46 (12801)	0.259 (158)	0.817 (498)	0.871	77	81 ± 7	7		
R22527	Avalanche Bay	3	20	1.46 (12801)	0.329 (1010	1.246 (382)	0.733	77	68 ± 8	11		
R22534	Discovery Bluff	1	25	1.32 (9539)	1.495 (943)	6.780 (4277)	0.883	2	51 ± 2 52 ± 3*	6	14.7 ± 0.14 (100)	1.4
R22570a	Devils Punchbowl	175	25	1.43 (10028)	0.407 (218)	1.818 (975)	0.910	59	56 ± 4	18	14.3 ± 0.33 (21)	1.5
R22570b	Devils Punchbowl		27	3.41 (23556)	0.257 (154)	2.674 (1600)	0.939	71	58 ± 5	10		
R22567	Cuff Cape	15	25	1.43 (10028)	0.367 (203)	2.050 (1135)	0.934	28	45 ± 4	20		
R22571a	Low Ridge, west of Cuff Cape	175	20	1.36 (11851)	0.603 (282)	2.704 (1265)	0.945	52	53 ± 4	26		
R22571b	Low Ridge, west of Cuff Cape		20	4.08 (3575)	0.357 (184)	5.841 (3014)	0.979	3	44 ± 3 62 ± 8*	19		
				South of Mackay Glacier (Inland of Granite Harbour)								
R22541	Red Ridge	481	12	1.32 (9539)	4.129 (1096)	10.43 (2770)	0.971	41	92 ± 3	10	13.1 ± 0.20 (100)	2.0
R22543	Killer Ridge, NE corner	450	25	4.08 (3575)	0.655 (204)	4.649 (1446)	0.999	92	101 ± 8	12		
R22548	Sperm Bluff, north flank	431	20	1.36 (11790)	0.853 (653)	2.557 (1958)	0.938	7	80 ± 4	26		
R22549	Sperm Bluff, south flank	396	18	1.36 (11790)	3.165 (1148)	8.401 (3047)	0.948	13	90 ± 3	81	12.8 ± 0.20 (100)	2.0
R22550	Cotton Glacier, north side	433	20	1.36 (11790)	0.623 (383)	1.896 (1153)	0.356	11	80 ± 5	18		
R22551	Miller Glacier, west side	503	24	1.33 (9539)	0.379 (375)	1.94 (1919)	0.815	10	46 ± 3	20	15.0 ± 0.13 (100)	1.3
R22555	Queer Mountain, north ridge	403	22	1.34 (9539)	1.651 (1027)	3.839 (2388)	0.971	3	101 ± 4 103 ± 6*	38	13.3 ± 0.20 (100)	2.0
R22556	Mount Sucss	650	23	1.36 (11790)	1.127 (467)	3.019 (1251)	0.834	4	89 ± 5 105 ± 5*	29	12.9 ± 0.21 (100)	2.1
R22557	Clare Range	995	20	1.36 (11790)	0.943 (551)	1.299 (759)	0.905	32	172 ± 10	12	12.5 ± 0.22 (100)	2.2
R22558a	Nunatak south of Redcliff Nunatak	458	21	1.36 (11790)	0.746 (277)	2.162 (803)	0.904	14	83 ± 6	2		
R22558b	Nunatak south of Redcliff Nunatak		20	4.08 (3575)	0.613 (282)	4.986 (2285)	0.994	88	89 ± 6	16		

total stratigraphic thickness above the break in slope (4.5-5 km) and a temperature of 130°C for the base of the apatite PAZ. This temperature of 130°C was based on the temperature at the base of the PAZ found in the Otway Basin of southeastern Australia [Gleadow and Duddy, 1981]. We now know that this temperature of 130°C is elevated due to the presence of chlorapatites, which are more resistant to annealing than fluroapatites [Green et al., 1986]. A temperature of ~110°C for the base of the PAZ established over a period of tens of millions of years, for more fluorine-rich apatites (e.g.,

TABLE 3. (continued)

Sample	Locality	Elevation m	Number of Grains	Standard Track Density ($\times 10^6$ cm^{-2})	Fossil Track Density ($\times 10^6$ cm^{-2})	Induced Track Density ($\times 10^6$ cm^{-2})	Correlation Coefficient	Chi Square Probability %	Age Ma	Uranium ppm	Mean Track Length µm	Standard Deviation µm
				South of Mackay Glacier (Inland of Granite Harbour) continued								
R22559a	Redcliff Nunatak	545	10	1.36 (11790)	0.769 (132)	3.372 (579)	0.990	2	55 ± 5 81 ± 9*	34		
R22559b	Redcliff Nunatak		20	4.08 (3575)	0.429 (147)	4.259 (1459)	0.984	7	72 ± 6	15		
R22560	West of Minnehaha Icefalls	275	31	1.35 (9539)	0.333 (247)	2.527 (1873)	0.793	6	31 ± 2	24	14.3 ± 0.24 (21)	1.1
				North of Mackay Glacier (Granite Harbour)								
R22506	Gregory Island	5	49	4.08 (3575)	0.161 (133)	1.902 (1567)	0.750	99	61 ± 6	6		
R22508	The Dreikanter, summit	556	20	1.25 (2188)	1.847 (369)	8.896 (1777)	0.841	9	46 ± 3	93		
R22514	The Dreikanter, base	15	25	1.43 (10028)	0.372 (234)	2.242 (1412)	0.910	4	42 ± 3 50 ± 5*	21	14.1 ± 0.29 (23)	1.4
R22561	Cape Archer	1	18	4.08 (3575)	0.186 (53)	2.381 (678)	0.805	43	56 ± 8	8		
R22562	Long Bluffs	1	20	4.08 (3575)	0.135 (63)	2.197 (1024)	0.817	68	44 ± 6	7		
R22563	Lion Island	15	20	1.36 (11851)	1.698 (891)	7.312 (3837)	0.991	63	56 ± 2	70	14.2 ± 0.15 (100)	1.5
R22566	Kar Plateau, NW corner	~530	20	1.36 (11851)	1.005 (624)	5.234 (3251)	0.958	11	46 ± 2	50	13.9 ± 0.19 (100)	1.9
R22716	Kar Plateau, NW corner	514	20	1.25 (2188)	1.077 (217)	5.506 (1109)	0.511	12	43 ± 3	58	14.1 ± 0.17 (100)	1.7
R22568	Kar Plateau, east end	33	21	1.36 (11851)	1.050 (561)	6.295 (3364)	0.946	6	40 ± 2	62	14.3 ± 0.10 (100)	1.0
R22569	Kar Plateau, west end	2	25	1.43 (10028)	0.564 (460)	3.365 (2745)	0.990	77	42 ± 2	32		
R22717	Mount Marston, summit	1247	20	1.25 (2188)	2.288 (1012)	5.758 (2547)	0.966	27	87 ± 4	60	13.2 ± 0.23 (101)	2.4

Values in parentheses are number of tracks counted. Standard and induced track densities measured on mica external detectors (g=0.5), and fossil track densities on internal mineral surfaces. Ages calculated using ζ=354 for dosimeter glass SRM612 [Hurford and Green, 1983]. Errors are given as ± one standard deviation. * Mean age, used where pooled data fail χ^2 test at 5%.

Durango apatite) is much more reasonable. Seiber [1986] found that apatites from most basement intrusive rocks have compositions similar to, or with even less Cl content than, Durango apatite. All apatites in this study come from the Granite Harbour Intrusives, hence the paleogeothermal gradient is calculated to be 20°-25°C/km. It is important to note that this estimate is for the late Cretaceous-early Cenozoic and is unrelated to independent measurements of geothermal gradients today. Higher geothermal gradients have been measured in some drill holes in the area of the TAM Front [Decker and Bucher, 1982] that are related to the effects of extensional tectonics, crustal thinning, and the associated alkaline volcanism. Even higher geothermal gradients have been estimated from mineral assemblages in crustal xenoliths from volcanic centers within the confines of the TAM Front. From these assemblages, Berg and Herz [1986] and Berg et al. [1989] determined that the present-day upper crustal geothermal gradient is between 50° and 100°C/km.

Gleadow et al. [1984] used a geothermal gradient of 30°C/km, based on heat flow measurements from a drill hole near Lake Vida (Figure 4), to estimate the depth at which the apatite age would go to zero and hence calculate the amount of uplift. Gleadow and Fitzgerald [1987] also used this as a subsidiary method to estimate the amount of uplift at Mount Doorly. Berg and Herz [1986] suggested that their increased estimate of the present-day geothermal gradient at the TAM Front may halve estimates of the rate of uplift suggested by the fission track data. However, only if the mineral assemblages in these crustal xenoliths were to show that in the late Cretaceous-early Cenozoic the geothermal gradient was significantly in excess of ~20°C/km would the fission track results conflict with the thermobarometric studies on the inclusions in the Cenozoic volcanics. The value of 30°C/km as used by Gleadow et al. [1984] actually, although not explicitly stated, related to a preuplift geothermal gradient (i.e., late Cretaceous). As shown in later studies [Gleadow and Fitzgerald, 1987] (this paper, see below), it is difficult to constrain the rate of uplift from the slope of the apatite age profiles below the break in slope. The method of determining the amount of uplift and denudation by reconstructing the stratigraphic section is independent of estimates of the geothermal gradient. A high present-day geothermal gradient does not therefore affect the calculation of the amount of uplift and the average uplift rate. In fact, recent models developed to account for the formation of the TAM [Fitzgerald et al., 1986; Stern and ten Brink, 1989] require a high present-day geothermal gradient and increased surface heat flow in the TAM Front.

Rate of Uplift

The amount of uplift is ~5 km at Mount Doorly and Mount England and ~6 km at the axis of maximum uplift (Mount Termination). Over the interval since the start of uplift and erosion (~60 Ma) the average uplift rate for the axis of maximum uplift is ~100 m/m.y. It is important to note this is an average value that could conceal phases of significantly higher and lower uplift rates and certainly does not imply that uplift was necessarily uniform since the early Cenozoic. In fact, no significant changes in apatite age with elevation can be observed for 500 m below the break in slope on the Mount England profile. Therefore the slope of the age profile below the break leaves the initial actual uplift rate poorly constrained. At Mount Doorly, the situation is very similar to that at Mount England with little significant change in age over 400

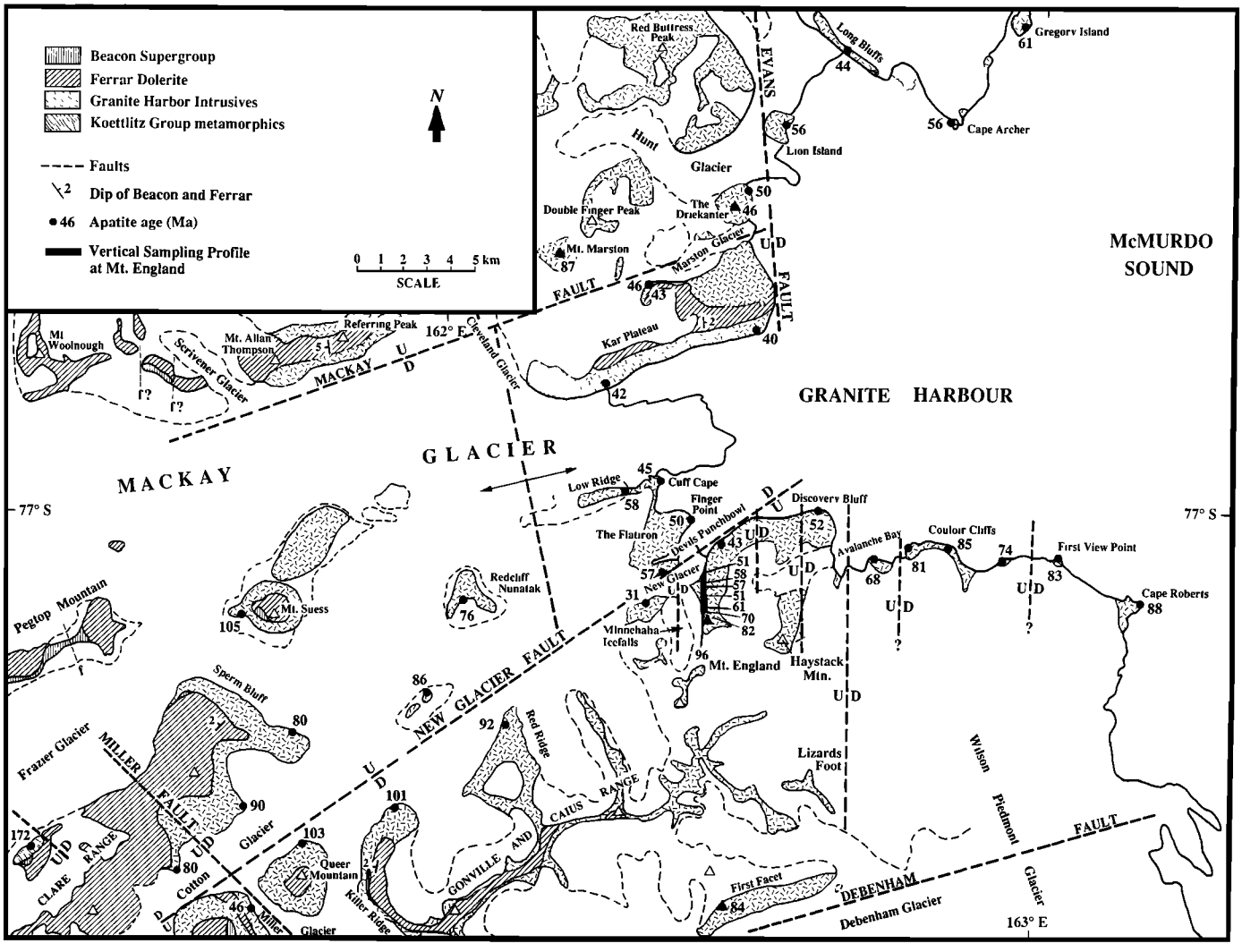

Fig. 13. Geologic map of the Granite Harbour area showing apatite ages and faults (dashed lines) determined from field evidence and the variation of ages.

m of elevation [Gleadow and Fitzgerald, 1987]. The lack of age variation suggests that the initial period of uplift and denudation was rapid (>100 m/m.y.).

Track length distributions from below the break in slope also support an initially rapid rate of uplift. The relative proportions of long and short lengths in a distribution can reveal the relative proportions of time that sample has resided at various temperatures [Gleadow et al., 1986a, b]. If a sample from just below the break in slope had cooled uniformly (implying a uniform rate of uplift) since ~55 Ma, then the length distributions would contain many more short tracks and have lower means (~13.5 μm) and larger standard deviations (~2.2 μm) as determined using the preferred annealing model of Laslett et al. [1987] and Green et al. [1989]. Application of this model together with the observed confined track length distributions constrains the uplift rate for the first 10-15 Ma, after initiation of uplift, to ~200 m/m.y.

In situ plant remains in the Dominion Range in the Beardmore Glacier area within glacially derived sediments of the Pliocene Sirius Formation, deposited by advances of the East Antarctic Ice Sheet over an already established mountain range, yield information about late Cenozoic glacial and climatic conditions, as well as the later uplift of the mountains [Webb et al., 1984, 1987; McKelvey et al., 1991]. Constraints placed by the elevation of the in situ woody stems initially suggested uplift of at least 1300 m in the last 2.5-3 m.y. [Mercer, 1986], but work in progress suggests that the amount of uplift since that time may be much less [D. Harwood, personal communication, 1990]. These data are not in conflict with the fission track data, which can only be used to establish the start and amount of uplift and place constraints on the initial and average rates of uplift. In all practicality the paleontological data and the fission track data look at the uplift of the TAM on different orders of magnitude. The fission track data look at the larger scale and do not and will not unravel all the complexities of late Cenozoic uplift. Rather, if the information is taken together, it means that the uplift of the TAM must have been episodic, with an period of rapid uplift in the early Cenozoic, little tectonic activity in the mid-Cenozoic, and then a more rapid period of uplift since the Miocene (Figure 16).

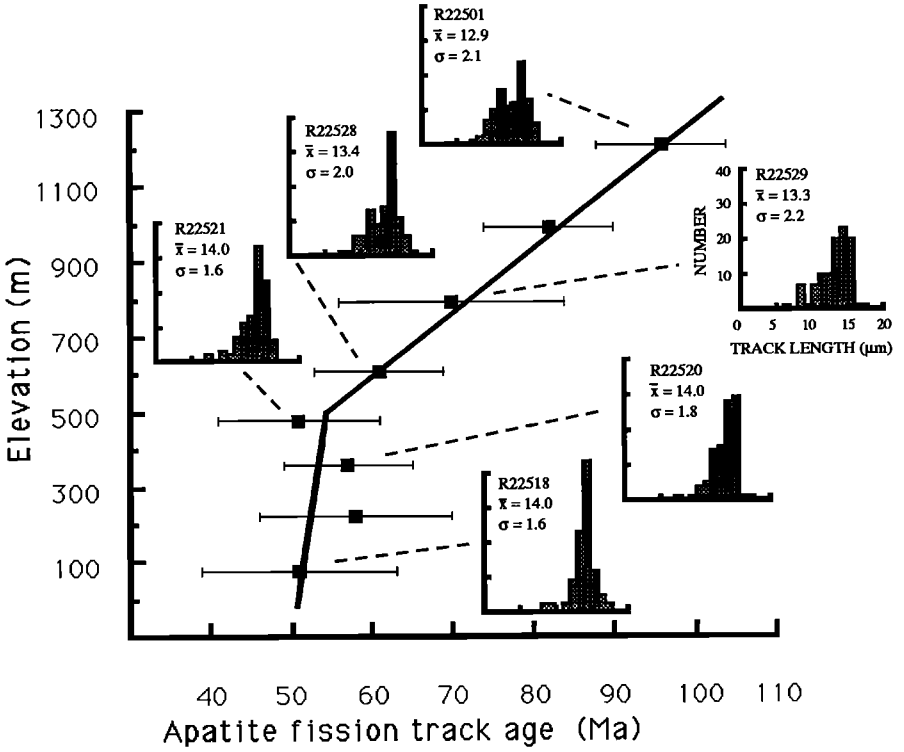

Fig. 14. Apatite ages versus sample elevation for results from the Mount England vertical profile. Note the break in slope at an elevation of ~500 m and ~55 Ma. Error bars are ±2σ. Confined track length distributions (Table 3) are plotted for a representative selection of samples. Plots are normalized to 100 tracks. Samples lying above the break in slope have significantly shorter lengths with larger standard deviations, reflecting considerable time spent in the PAZ where tracks are shortened. Mean lengths from samples below the break are longer and have smaller standard deviations, reflecting rapid cooling from temperatures above the track retention zone with a relatively short residence in the PAZ.

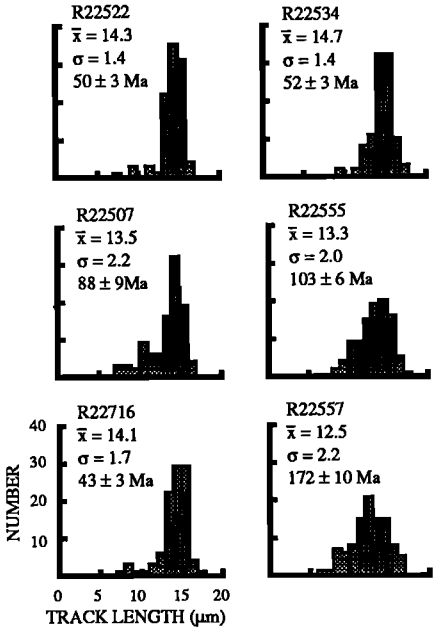

Fig. 15. Track length distributions for a number of representative samples from the Granite Harbour region (Table 3).

STRUCTURAL AND TECTONIC INTERPRETATION OF THE FIELD AREAS

Apatite ages on the upper part of the age-elevation profile (above the break in slope) vary significantly with sample elevation and can be used as tectonic indicators of paleodepth in the preuplift crust. The much steeper gradient in relation to the uncertainties in measured age below the break in slope precludes the precise use of apatite ages from this level as structural markers. Ages <~55 Ma in the Granite Harbour region and <~50 Ma in the Wilson Piedmont Glacier area are considered to lie beneath the break because track length distributions of these samples (Tables 2 and 3) are indicative of rapid cooling. Length distributions for samples older than these ages are indicative of more complex thermal histories and thus indicate that these samples lie above the break in slope.

The Wilson Piedmont Glacier area

The Mount Doorly-Mount Allen ridge system: The natural reference surface of the basement dolerite sill delineates the structure of the TAM Front (Figure 9) better than anywhere else yet found. The step faulting along the Mount Doorly-Mount Allen ridge system characterizes the nature of the faulting across the TAM Front, and the presence of dolerite at Kolich Point [Gleadow and Fitzgerald, 1987] (Figure 4) places constraints on the magnitude of the faulting. The total offset across the TAM Front from Mount Termination to the

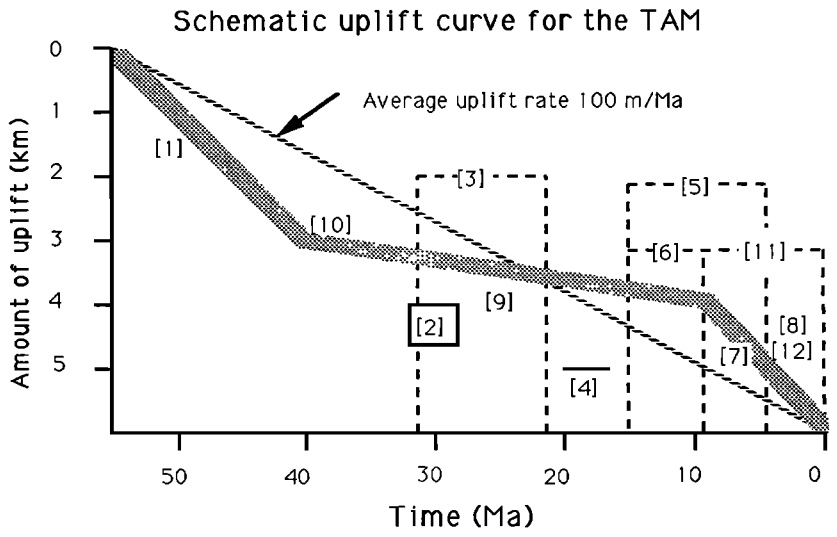

Fig. 16. Schematic uplift curve for the TAM (broad stippled line) since the inception of uplift at ~55 Ma illustrated for a point near the axis of maximum uplift. This curve is based on fission track modelling and other geological evidence as presented below. The curve shows an initially rapid period of uplift in the early Cenozoic followed by a period of little apparent tectonic activity in the mid-Cenozoic and then a more rapid period of uplift since the Miocene. A uniform rate of 100 m/m.y. is also shown for comparsion (broken line). 1, modelled fission track data: initial uplift rate rapid, ~200 m/m.y. for the approximate period 55-40 Ma. 2, Drewry [1975]: the mountains 1500-2000 m lower in the late Oligocene (~30 Ma). This point plots lower than the uplift curve because it relates to topographic elevation of the mountains and not uplift. 3, Harwood [1986]: MSSTS-1 drill hole offshore off Butter Point (Figure 3) for the period 31-21 Ma had a slow sediment accumulation rate of 20 m/m.y. inconsistent with more rapid uplift in the adjacent mountains. Assumption that sedimentation rate is approximately equal to the uplift rate. 4, Stump et al. [1980]: at least 900 m of relief at 15-19 Ma. This point plots lower than the uplift curve because it refers to relief and sets a minimum value for the amount of uplift. 5, Webb [1986]: offset between Pliocene sediments for MSSTS-1 drill hole (offshore, Figure 3) and DVDP-8-10 drill holes (onshore at mouth of Taylor Valley) was used to determine displacement rates of 18-36 m/m.y. between these two areas for the period 2-4 Ma, and a displacement rate of ~95 m/m.y. between MSSTS-1 and the central Wright Valley for the same period of time. 6, Denton et al. [1984]: at least two periods of overriding of the TAM by the East Antarctic Ice Sheet, at least one before the period 9-15 Ma, and at least one after. 7, Barrett [1975]: a major change in pebble type at DSDP site 270 after the Miocene interpreted as a consequence of glacial downcutting related to uplift. 8, information from the Sirius Formation [Webb, 1972; Webb and Wrenn, 1982; Wrenn and Webb, 1982; Webb, 1986; Mercer, 1985; D. Harwood, personal communication, 1990]. 9, Barrett [1986]: the lower 40 m of the MSSTS-1 core, between 31 and 28 Ma records a marine regression culminating in an unconformity followed by till deposition. Harwood [1986] concludes that this sequence and existing isotopic and eustatic evidence supports a model of climatic decline and significant ice volume increase at ~ 30 Ma. This is diagramatically modelled as slowing uplift. 10, the first presence of significant ice in Antarctica [Kerr, 1984; Barrett, 1987; Barron et al., 1989] may slow the uplift. Complete ice sheet overriding of the mountains may depress the mountains ~500 m [Smith and Drewry, 1984], with subsequent accelerated uplift after removal of the ice. 11, Behrendt and Cooper [1991]: rapid uplift since early or middle Pliocene because of youthful appearance of rift shoulder, Holocene fault scarps, and comparsion to other rift shoulder uplift rates. 12, Wilch et al., [1989]: maximum uplift rates of 137-397 m/m.y. since 3 Ma determined using $^{40}Ar/^{39}Ar$ ages on cinder cones in Taylor Valley and dividing the lowest elevation of in situ subaerially erupted volcanics by the age.

McMurdo coast is ~2000 m, assuming an average westerly dip of 2°-3° for the individual fault blocks persists across the fault zone. Of that, ~1000 m is taken up by observed faults present along the Mount Doorly-Mount Allen ridge system (Figure 9). Taking into account the 2°-3° dip, all of the apatite ages along this ridge system agree exceptionally well with the displacements determined from offset dolerite sills. The position and offset of another fault, just to the east of Mount Termination, can be delineated from the fission track data alone.

It is difficult to ascertain whether a fault is present between Mount Termination and Mount Theseus (Figure 11). If Mount Termination was higher in elevation, then the base of the basement dolerite sill would probably be present at an elevation of ~1600 m. If no fault was present between the two peaks, and taking into account a 2°-3° westerly dip, then the basement dolerite sill should occur at Mount Theseus at an elevation of ~1300 m. A dolerite sill does occur on the eastern ridge of Mount Theseus, with its base at an elevation of 1600 m. This

is, however, the peneplain dolerite sill, because the basement sill pinches out locally just to the west. Further west in the Wright Valley the basement sill usually parallels the peneplain sill but is ~300 m lower. This would mean that the basement sill, albeit thinned, would probably occur at an elevation of ~1300 m at Mount Theseus, as expected. Therefore it is unlikely that any major fault exists between Mount Theseus and Mount Termination. Mount Termination thus represents the point of maximum uplift (the structural high) on an east-west transect line through the TAM in this area.

Other localities: The elevation difference between the two samples on Hansen Ridge (Figure 11) is not sufficient to account for the age difference, given the gradient of the profile above the break in slope (~15 m/m.y.). Furthermore, the age variation exceeds what we would expect to see if Hansen Ridge was tilted 2°-3° to the west, but it can be explained if Hansen Ridge has a westerly dip of 5°-6°. While somewhat necessarily speculative, this increase in dip to the fault blocks across the TAM Front follows the apparent trend of increasing westerly dip of the individual fault blocks down the Mount Doorly spur. The fission track data neither confirm nor deny the presence of a fault between the western end of Hansen Ridge and Blessing Bluff (Figure 11), as the ages lie well within error limits. However, given the nature of the TAM Front, it is likely that a fault does exist through this quite distinct gap. A fault must exist between Hansen Ridge and the coast to account for the difference between the 69 ±3 Ma age at the east end of Hansen Ridge and the ~96 Ma age at Spike Cape. Assuming a westerly dip of 5°, an offset of ~1000 m (± 200 m) down to the east is required to explain this age difference.

The ages along Staeffler Ridge are similar to those at similar elevations along the Mount Doorly spur and thus provide no evidence for an east-west trending fault along the Greenwood Valley as was tentatively suggested from field evidence. A fault, or faults, is likely to be present between Blessing Bluff (83 ±9 Ma) and the middle of Staeffler Ridge (73 ±5 Ma), where a westerly dip of 2°-3° would imply an offset of 700 ±250 m, downthrown to the east. The positions of these faults are likely to lie in similar positions to those along the Mount Doorly spur, assuming they continue across Greenwood Valley. The apatite ages from Pond Peak tell us little, except the samples are from a similar crustal level to those from Staeffler Ridge and the Mount Doorly spur. The sample from the Olympus Range (R22677, 155 ±9 Ma) has a smaller mean length than other samples from this area (Figure 10). This distribution is similar to those of a similar age from the Mount Jason vertical profile [Gleadow and Fitzgerald, 1987] and is indicative of a longer time period spent at higher temperatures, most likely reflecting the relaxation of isotherms and reestablishment of a PAZ after heating accompanying Jurassic magmatism.

The step-faulted structure at Mount Newall (Figure 12) is similar to that seen along the Mount Doorly spur (Figure 9). There is a total displacement of ~700 m between the dolerite capping the summit of Mount Newall and the dolerite cropping out along the northeast ridge. Using the apatite ages, it is possible to break up this displacement into two faults, one of ~400 m displacement and the other of ~300 m, as shown when the ages are plotted against elevation (Figure 17). On this diagram, the vertical profile (Mount Newall (S)) plots at the lowest elevation as it lies on the downthrown side of these two faults. Samples (with similar apatite ages) that come from blocks that are progressively upthrown to the west therefore

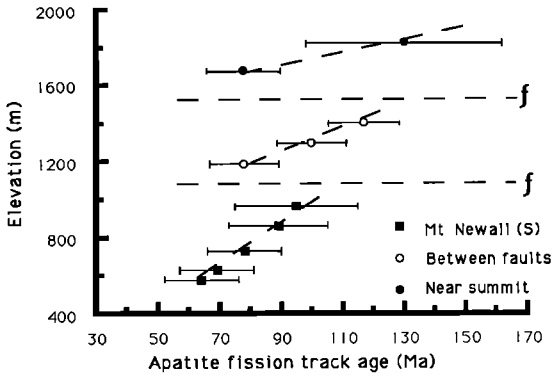

Fig. 17. Apatite age profile from Mount Newall showing data points down the northeastern ridge system and how individual profiles have been offset by faulting. Apatite ages and the positions of the faults are shown in Figure 12. Samples R22605 and R22606 (Figure 6) lie near the summit. Samples R22607-R22609 lie between the two faults. The Mount Newall (S) profile is from the southern spur off the northeast ridge (samples R22610-R22614). Error bars are ±2σ.

plot at higher elevations. From this diagram it is possible to calculate the relative offset across the faults.

The two vertical sampling profiles from Mount Newall (Figure 6) show a strong correlation of age with elevation and define gradients of ~15 m/m.y. (Figure 18). The offset between these two profiles is due either to faulting or, if they lie on the same tectonic block, to a dip of 1°-2° to the south over the intervening 5 km. No fault is evident between these two profiles, and a southerly tilt is consistent with the pattern of decreasing age to the south for the youngest marine sediments in Dry Valley Drilling Project cores from the Wright and Taylor valleys [Wrenn and Webb, 1982]. A break in slope probably exists near the base of the profile from the north flank at ~50 Ma. A break is also shown for the southern spur data at the same age as the other two profiles but lying at a lower elevation (Figure 19). A fault exists between Kingpin (Figure 11) and Mount Newall. The age of 93 ±6 Ma from Kingpin is at the same elevation as an age of ~78 Ma from the lowermost fault block off the northeast ridge of Mount Newall. This age difference, plus the inferred westerly dip (2°-3°), gives an offset of ~400 m (±100 m), down to the east.

Apatite ages along the southern end of the Wilson Piedmont Glacier, from Hjorth Hill to Mount McLennan are similar (Figure 11), but when viewed with respect to elevation, and incorporating the westerly dip of the fault blocks, a number of faults are required (Figure 20). Faults between Mount McLennan and Mount Falconer and between Mount Coleman and Hjorth Hill have offsets of ~600 m (±150 m) and ~350 m (±150 m), respectively. If the apatite age at Cape Bernacchi is the same as the other coastal samples (~96 Ma) (Figure 11), then the offset between Hjorth Hill and the coast would be ~1000 m, similar to that estimated between Hansen Ridge and Spike Cape. An east-west trending fault probably exists between Kingpin and Mount Coleman and Mount Falconer. Taking into account the 1°-2° southerly dip of the fault block as determined above, the apatite age of 93 ±6 Ma that occurs at Kingpin at an elevation of 735 m should occur at an elevation of ~400 m between Mount Coleman and Mount Falconer some 12 km to the south. Extrapolating down from 93 Ma, using the

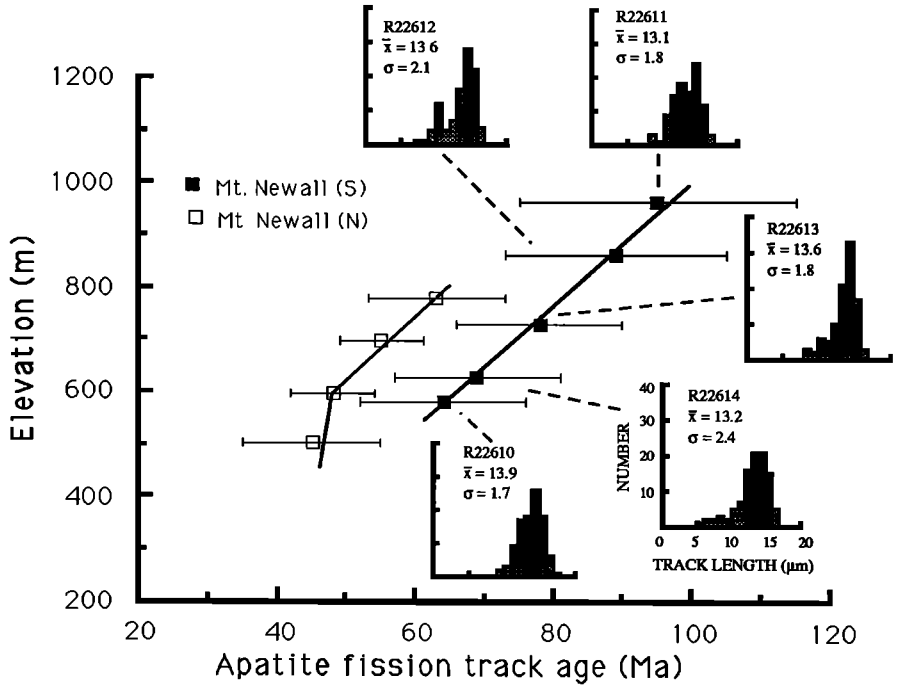

Fig. 18. Apatite age versus elevation for the two vertical sampling profiles off Mount Newall. Mount Newall (N) is the profile taken by Gleadow and Fitzgerald [1987] on the northern flank of the Mount Newall massif (Figure 6). Note the break in slope on the Mount Newall (N) profile. Mount Newall (S) is from the southern spur off the northeast ridge and includes samples R22611-R22614 (Figure 6) plus sample R22610 from the end of the northeastern ridge. The apatite age from sample R22610 lies on the same elevation versus age trend as the other four samples, indicating that no major faults lie between these two sampling areas. Error bars are ±2σ. Length distributions (with mean length and standard deviations in microns) are also plotted for this profile.

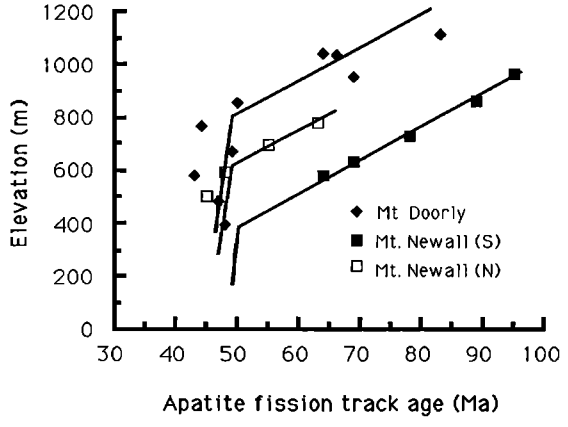

Fig. 19. Apatite age profiles from Mount Doorly and Mount Newall. The position of the break in slope on the two Mount Newall profiles is assumed to occur at the same age as the Mount Doorly profile. The Mount Doorly profile rather than the Mount England profile is used here because of its proximity to the Mount Newall massif. Mount Newall (N) is the profile taken by Gleadow and Fitzgerald [1987] on the northern flank of the Mount Newall massif (Figure 6). Mount Newall (S) is from the southern spur off the northeast ridge (samples R22610-R22614). Error bars have been omitted to avoid clutter. The offset of the profiles indicates a 1°-2° southerly tilt of the fault block containing these profiles.

gradient of 15 m/m.y. (as determined from the age profile at Mount Doorly and Mount England), an age of ~70 Ma should occur at an elevation of ~50 m between Mount Coleman and Mount Falconer. However, the apatite age of ~70 Ma between these two peaks (Figure 20) is at an elevation of ~800 m, which implies the presence of a fault between Kingpin and Mount Coleman and Mount Falconer, with an offset of ~750 m (±180 m), up to the south.

The Granite Harbour Region

The south side of Granite Harbour: The pattern of apatite ages across the south side of the harbour (Figure 13) gives information on the location of, and displacements across, a number of faults lying within the confines of the TAM Front (Figure 21). The total relative offset between Mount England and Cape Roberts is ~1800 m downthrown to the east. This is calculated from the ~1100 m (±150 m) vertical difference between the age of 88 ±9 Ma at Cape Roberts and approximately the same age on the Mount England profile (Figure 14). An additional ~700 m of displacement is estimated due to the dip of the fault blocks across the TAM Front, which is assumed to be 2°-3° to the west, as observed elsewhere. Of this ~1800 m, there is about 1000 m (± 150 m) displacement between Mount England and Avalanche Bay. This is in part taken up by the fault just west of Avalanche Bay, but another fault is also likely between Mount England and Discovery Bluff as marked by the distinct topographical break there (Figures 8 and 21). Another ~800 m offset, down to the east, is therefore required between Avalanche Bay and Cape Roberts. This is

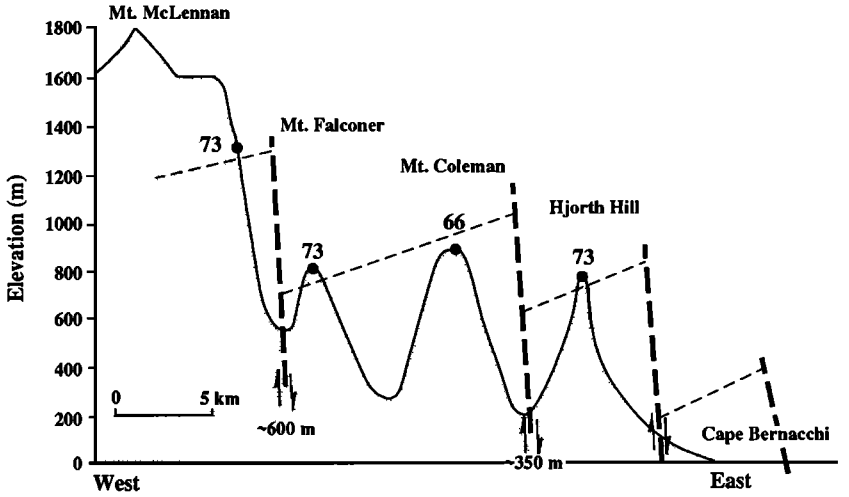

Fig. 20. Simplified cross section across the southern end of the Wilson Piedmont Glacier, from Mount McLennan to Cape Bernacchi (Figures 4 and 11), showing the positions of, and displacements across, faults (thick dashed lines) that have been inferred from the apatite fission track data. The idealized structure across the mountain front is depicted by the ~70-Ma isochron (thin dashed lines).

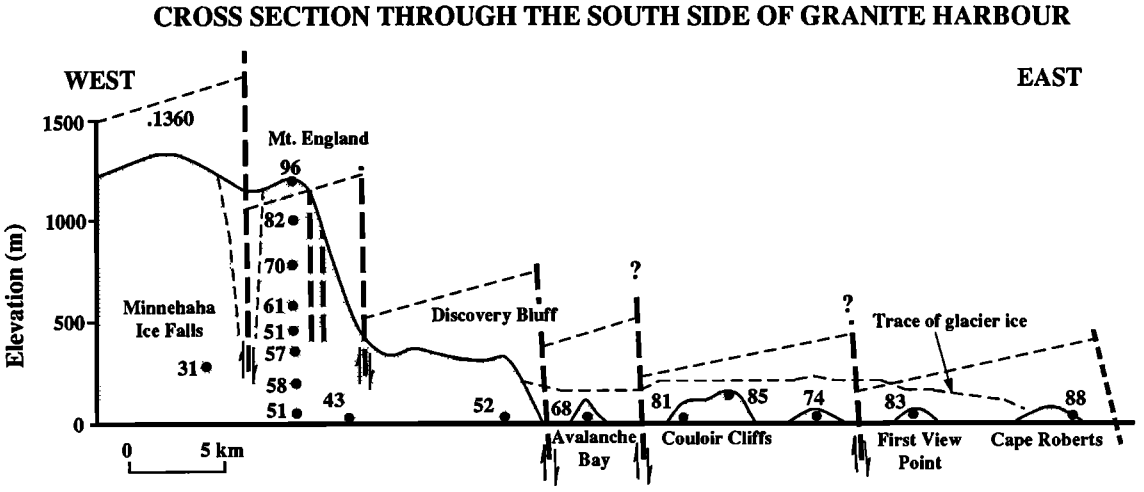

Fig. 21. Simplified cross section along the southern shores of Granite Harbour from spot height 1360 to Cape Roberts (Figures 7 and 13), showing the probable location of, and approximate displacement, across faults (thick dashed lines) across the TAM Front. The idealized structure across the mountain front is depicted by the ~95-Ma isochron (thin dashed line).

probably taken up on faults that lie to the west of Couloir Cliffs and to the west of First View Point where there appear to be slight differences in the apatite ages, even though they are within error limits. The two faults plotted on Figure 21 between Avalanche Bay and Cape Roberts have therefore been arbitrarily placed on the east side of Avalanche Bay and to the west of First View Point where there is the greatest apparent difference in age between adjacent samples.

Inland of Granite Harbour: To the west of Minnehaha Icefalls an age of 31 ±2 Ma suggests a fault between there and Mount England, downthrown to the east (Figure 21). The displacement on this fault is hard to estimate because the 31 Ma age lies well below the break in slope, but it is likely to be at least several hundred meters. To the west, the structure of the mountains appears to be relatively simple. The peneplain dolerite sill dips gently westward from spot height 1540 (Figures 7 and 8) until it is faulted across the Miller Glacier. The apatite age of 46 ±3 Ma on the western side of the Miller Glacier compared to an age of 103 ±6 Ma at Queer Mountain is consistent with the displacement of 300-400 m (up to the west) determined from the offset in the dolerite sills (Figure 8).

The interpretation of the structure from the fission track results in this region is less well constrained from this point on. The question was posed earlier as to whether a fault exists up the New Glacier. Unfortunately, apatite ages at the base of Mount England and from The Flatiron (Figure 13) lie below the break in slope and are thus unreliable as tectonic markers. However, from the presence of a dolerite sill on the Kar Plateau and lack of any dolerite on Mount England it seems conclusive that a fault, upthrown to the south, does occur between these

two localities. As previously suggested, this fault most likely runs up the New Glacier and is called the New Glacier fault.

Ages from Sperm Bluff to Redcliff Nunatak (Figure 13) are slightly younger than ages from equivalent elevations at Queer Mountain, Killer Ridge, and Red Ridge, which lie to the south, across the New Glacier fault. This suggests two things, either the dip of the fault block is to the southeast, which is the opposite of the dolerite, which dips west to northwest at 2°-3°, or the northwest side of this fault is upthrown. The base of the dolerite sill capping Queer Mountain is at an elevation of ~900 m, similar to that at the eastern end of Sperm Bluff. However, taking into account the west to northwest dip of the dolerite, the dolerite at Sperm Bluff should be 100-200 m lower in elevation than that at Queer Mountain. Therefore the northwest side of this fault may be upthrown ~100-200 m. This scenario poses a problem, however, because further to the east near Mount England the north side of the New Glacier fault is downthrown. This dilemma may be solved if it is remembered that a north-south trending hinge line up the Cleveland Glacier has already been suggested on the north side of the MacKay Glacier. This hinge line probably extends south across the MacKay Glacier, and the structure may be as simple as it is to the north, where the blocks dip to the east, east of the hinge, and to the west, west of the hinge. This explanation accounts for the distribution of apatite ages and explains the apparent opposite senses of displacement at different ends of the New Glacier fault. In fact, this hinge line is coincident with, and hence represents, the axis of maximum uplift (as projected north from Mount Termination) inland of the Granite Harbour area.

The Miller fault crosses the New Glacier fault near the Cotton Glacier (Figure 13). West of the Miller fault and north of the New Glacier fault an age of 80 ±5 Ma suggests that this area is downfaulted relative to the south side of the New Glacier fault, where an apatite age of 46 ±3 Ma was obtained, and upthrown with respect to the eastern side of the Miller fault, where the apatite age is 90 ±3 Ma. The latter displacement is estimated at 250 ±100 m. The two ages from Sperm Bluff (from similar elevations), 80 ±4 Ma on the northeast side and 90 ±3 Ma on the south flank, are consistent with the general northwest dip of the fault block as shown by the dip of the dolerite. Further to the west again, basement rock appears upthrown against the dolerite at sample site R22557. Sample R22557 has a shorter mean length (12.5 μm) than the other samples from this region (Figure 15), indicating a greater degree of partial annealing. This track length distribution could have been brought about by more time spent within the PAZ, in which case an apatite age of 172 Ma is too old if the sample was reset to zero at ~180 Ma (i.e., given the percentage of partial annealing this sample has undergone to get this length distribution, we would expect a somewhat younger age if it had been reset to zero at ~180 Ma). A more likely explanation is that a component of partially annealed pre-Jurassic tracks is present (i.e., the sample was only partially annealed by Jurassic heating).

The north side of Granite Harbour: Most of the ages lie near or below the break of slope (Figure 13) and are therefore of little use as tectonic markers. There is no age variation over 550 m of elevation at The Dreikanter. Ages on either side of the MacKay fault show no significant variation, even though we know there has been at least 800 m of offset across this fault on field evidence. There is no age variation across the north-south trending Evans fault. Similarly, ages across the mouth of the MacKay Glacier and in the Cuff Cape area give no information on the structure, although, in general, they do increase very slightly to the south, perhaps indicating that this fault block is tilted up to the north. Ages from Lion Island to Gregory Island indicate that a deeper crustal level is exposed on the northern side of Granite Harbour than on the southern side. It is likely that the mountain front is step faulted as it is to the south across the harbour (see Figure 21), but the fission track data give no definitive clues as to the location of any of these faults. The only age on the north side of Granite Harbour that clearly lies above the break in slope is from Mount Marston (87 ±4 Ma, 1247 m), indicating that this level resided at a similar structural level as the top of Mount England (1205 m) prior to uplift.

Tectonic Summary

The overall structure of the McMurdo Sound area of southern Victoria Land is defined by block faulting (Figure 22) and in the area discussed can be envisaged as one large westerly tilted fault block or flexure (Figure 23). To the west the fault block disappears under the East Antarctic Ice Sheet and to the east it is bounded by the TAM Front (a zone of north-south striking normal faults). The fault block is bounded to the north by a graben through which the Mackay Glacier flows and to the south by the Ferrar fault. Differences in the elevation of the Kukri Peneplain on either side of the Ferrar Glacier in the vicinity of Sentinel Peak indicate that the south side of the Ferrar fault is downthrown ~300 m. Within the fault block other east-west striking transverse faults also occur. Examples of these are the Debenham fault (Figure 7), the small fault north of Mount Doorly (Figure 5), the fault between Kingpin and Mount Coleman (Figure 11), and possibly the fault just south of Lake Vida in the Victoria Valley (Figure 22) determined from an offset apatite age profile [Gleadow et al., 1984].

The throw of longitudinal (north-south striking) faults across the TAM Front is generally down to the east, but in places small antithetic faults with a displacements of ~50 m are also present. Displacements observed from offset dolerite sills for longitudinal faults downthrown to the east vary from 40 to ~700 m. Fission track evidence has been used to confirm some of these and to detect a number of other faults that lie mainly within the ice-covered confines of the Wilson Piedmont Glacier, but also along the Mount Doorly spur (Figure 9), at Mount Newall (Figure 12), and along the southern end of the piedmont (Figure 20). The westerly dip of individual fault blocks may increase eastward across the TAM Front, perhaps indicating some rotation of the blocks on listric faults. North-south striking longitudinal normal faults appear to be at an acute angle to the trend of the axis of maximum uplift (Figure 23). These faults therefore cannot persist from Granite Harbour to the Ferrar Glacier. Instead, they appear to be offset by the east-west trending transverse faults. It is possible that more transverse faults exist in the study area, for example in the Victoria Lower Glacier, which would then neatly divide up the area between Granite Harbour and the Ferrar Glacier into four equally sized blocks. The angle of the longitudinal faults to the axis of maximum uplift is indicative of a dextral component to the primary east-west directed extension in the Victoria Land Basin (Figure 24). By inference, structures that delineate Cenozoic extension in the Victoria Land Basin should also have a dextral component.

Uplift at Mount Doorly based on a reconstructed stratigraphic profile is ~5 km [Gleadow and Fitzgerald, 1987], as is uplift calculated for Mount England. Inland from Mount Doorly is the NNW trending axis of maximum uplift (through Mount Termination), where uplift is ~6 km. This axis of maximum uplift for the Granite Harbour-Ferrar Glacier area is

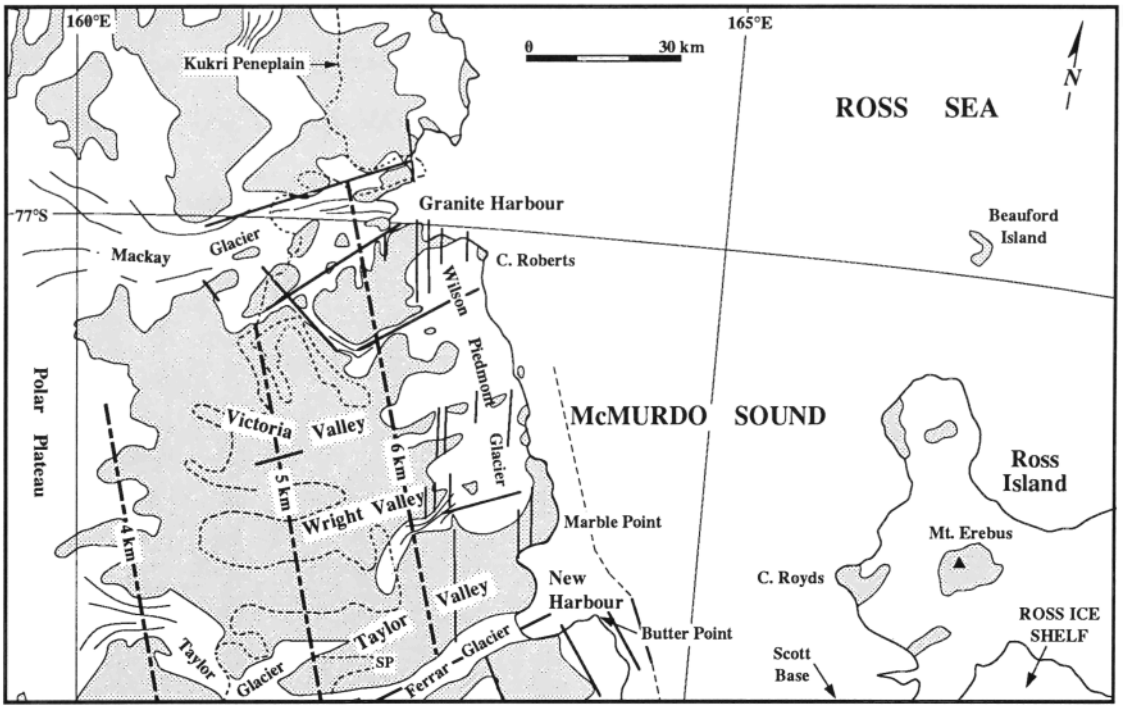

Fig. 22. Tectonic summary map of southern Victoria Land showing the position of known onland (thin solid lines) and offshore faults (thin solid lines, dashed where inferred, from Bennett and Sissons [1984] and McGinnis et al. [1983]). Also shown is the trace (where it crops out) of the Kukri Peneplain (modified slightly from Warren [1969]). The axis of maximum uplift (~6 km) between Granite Harbour and the Ferrar Glacier, the ~5 km and ~4 km uplift contours are also shown. SP is Sentinel Peak.

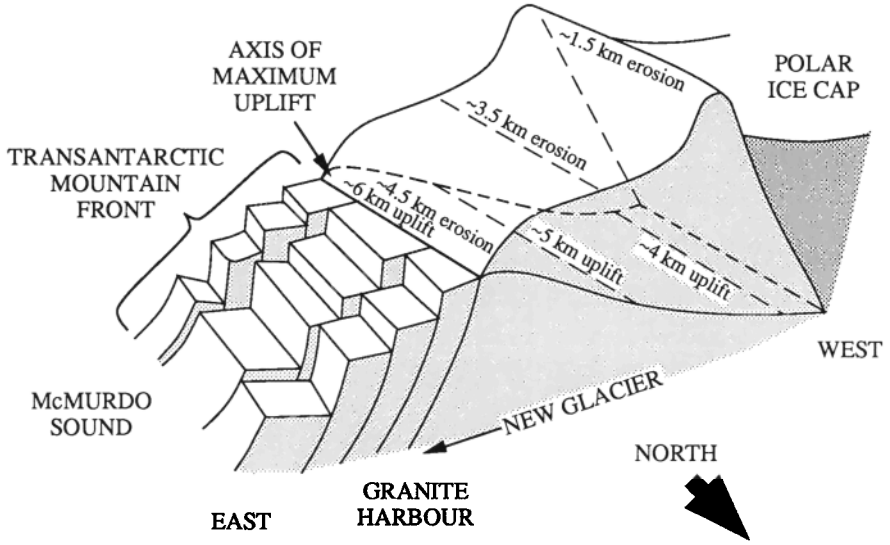

Fig. 23. Idealized block diagram of the structure of the TAM between Granite Harbour and the Ferrar Glacier showing the faulted TAM Front and uplift and erosion contours. Note that the north-south trending longitudinal faults are at an angle to the axis of maximum uplift, indicative of a dextral component to the dominantly east-west extension.

indicated by the ~6 km uplift contour (Figure 22). Also shown are the ~5 km and ~4 km uplift contours defined by the dip of the strata to the west and the artifical reference surface generated by the fission track data. The axis of maximum uplift has been extended north to Granite Harbour where it is coincident with a hinge line across the MacKay Glacier. There the block to the east of the hinge line is tilted to the east, and the block to the west of it is tilted to the west. Just east of the axis of maximum uplift at Mount Termination the dolerite also dips to the east (Figure 9) before reverting to its usual westerly dip.

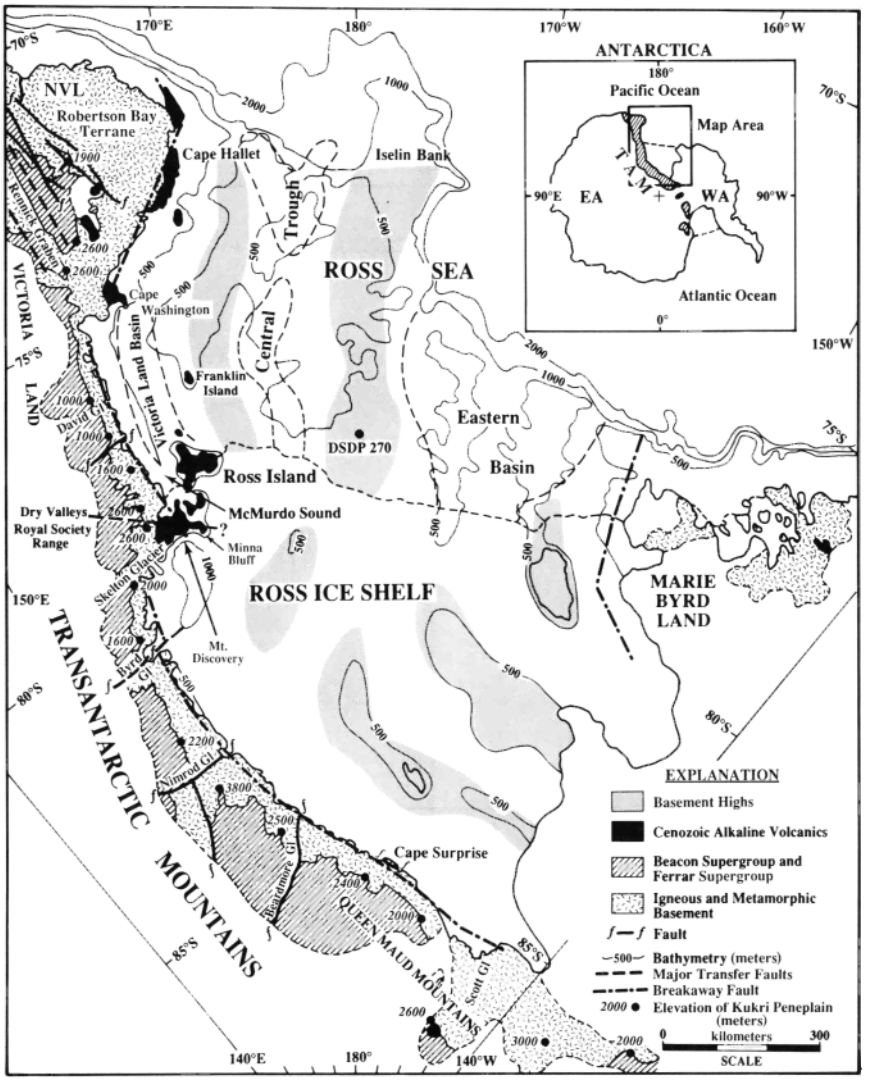

Fig. 24. Map of the TAM in the Ross Sea Sector showing the position of the suggested upper plate breakaway as marked by the TAM Front along the coastal edge of the TAM and the suggested lower plate breakaway near the Marie Byrd Land coast. Possible major transfer faults have been marked on the TAM Front at the Byrd Glacier and north of the Skelton Glacier. The trend of the Rennick Graben is not connected to the trend of the Victoria Land Basin, although they may have been connected prior to uplift of an intervening block. Basement highs in the Ross Embayment have been inferred from the bathymetry [Hayes and Davey, 1975; Craddock, 1982; Robertson et al., 1982] and sediment isopachs [Davey et al., 1983] of the Ross Sea.

This implies that the axis of maximum uplift may not be the angular edge of a large fault block (as in Figure 9) but instead may be gently folded at the hinge line before being step faulted down to the McMurdo coast (Figure 23).

Mount England lies within the confines of the TAM Front so the axis of maximum uplift which marks the edge of this flexure lies just to the west of the Minnehaha Icefalls. West of the axis the mountains are faulted in a number of places, defining the existence of other fault blocks. This is particularly evident where the Miller fault crosses the New Glacier fault. Along the south side of Granite Harbour the faulted nature of the TAM Front is evident from the fission track results (Figure 21). On the north side of the harbour, the same faulted mountain front is very likely, but the fission track results do not allow any constraints to be placed on the positions or displacements of any faults. Indeed, the fission track results there are a good example of the lack of tectonic control given by apatite ages from below the break in slope. The Mackay Glacier graben is bounded to the north by the Mackay fault and to the south by the New Glacier fault. Just beyond the mouth of Granite Harbour, Behrendt et al. [1987] (in LeMasurier and Thomson, [1990]) have suggested the presence of a submarine volcano defined by multichannel reflection profiles and shortwavelength magnetic anomalies. This, the Barrett Submarine Volcano, may lie at the intersection of offshore longitudinal faults and the transverse faults (Mackay and New Glacier faults), perhaps within the confines of the Mackay Glacier graben. Kyle and Cole [1974] suggest that many of the volcanoes in the Erebus Volcanic Province lie along or at the intersection of faults.

THE TAM AS AN UPPER PLATE MARGIN

The architecture of the TAM typifies the features of an upper plate passive mountain range as defined by Lister et al. [1986]. The adjacent extensional region of the Ross Embayment has the characteristics of a lower plate margin. Upper plate margins are relatively simple and tend to be narrow, commonly having passive-margin mountains with fairly widely spaced, steeply dipping normal faults that have small components of horizontal movement compared to relatively large vertical components and that step fault the basement down toward the locus of extension. Lower plate margins are generally more highly structured, due to remnants of deformed upper plate above a detachment fault, and are typified by rotated tilt blocks and half grabens overlain by gently dipping semicontinuous strata of the postextension, thermal subsidence or sag phase. These generic descriptions fit the general characteristics of the TAM and the Ross Embayment, with the TAM Front representing an upper plate breakaway zone and Marie Byrd Land possibly representing a lower plate breakaway. Extended crust underlies the sedimentary basins between the two breakaways.

The Victoria Land Basin (Figure 24), bounded on its western side by the uplifted TAM and to the east and north by a shallow basement platform, is a broad half graben filled with up to 14 km of subhorizontal strata [Cooper et al., 1987]. The strata are offset by many small normal faults, some of which are growth faults [Cooper and Davey, 1985]. Coincident with a central bathymetric trough in the basin is a central rift that has been created by syn-depositional faulting, along which lie submarine volcanic centers [Cooper and Davey, 1985]. Volcanic rocks of a similar composition also crop out at places on the western margin of the basin (the eastern flank of the TAM). It is probable that deformed prerift sediments, that is, remnants of the upper plate represented by strata of the Beacon Supergroup and Ferrar Dolerite, exist at the bottom of this basin, something that Cooper et al. [1987] also consider likely based on seismic stratigraphy. Cooper et al.'s [1987] preferred model suggests that initial basin development commenced sometime between middle Jurassic and early Cretaceous. Basin development was followed by sediment infilling until post-Eocene extension resulted in the superposition of the younger central rift, 50-60 km wide, consisting of a faulted graben (25-35 km wide) and an intruded arch (25-40 km wide). This later phase of deformation is believed to be responsible for most of the deformation in the sediments of the Victoria Land Basin [Cooper et al., 1987], as well as being coeval with the major uplift of the TAM [Fitzgerald et al., 1986].

Two other main basins exist in the Ross Embayment, the Central Trough and the Eastern Basin [Davey et al., 1983]. These are both shallower (maximum of 7 km of strata) and simpler in structure than the Victoria Land Basin; they both lack a central rift and any known volcanic centers [Hinz and Block, 1983; Davey at al., 1983], but nevertheless also appear to have formed in an extensional environment. In the Eastern Basin, most sedimentation and therefore presumably most subsidence, postdates the late Oligocene. Remnants of the upper plate may also underlie the Central Trough and Eastern Basin, but these remnants are unlikely to be present on the highly block-faulted basement highs [Cooper et al., 1987] that separate the basins of the Ross Embayment (Figure 24). These basement highs may be bowed up parts of the lower plate, analogous to metamorphic core complexes, and indeed the presence of calc-silicate gneiss, complete with a foliation and chlorite alteration [Ford and Barrett, 1975], is consistent with this idea, although it by no means proves it.

The similarity of the TAM and Ross Embayment with the Basin and Range Province of the western United States [e.g., Crittenden et al., 1980] and the East African rift system [e.g., Rosendahl, 1987] has been noted by geologists for many years. In the western United States, the Colorado Plateau-transition zone (Wasatah Front)-Basin and Range Province configuration corresponds to the TAM-TAM Front-Ross Embayment. However, unlike the Basin and Range Province, the structure and age of the sediments and underlying basement rocks of the Ross Embayment remain poorly constrained.

LONGITUDINAL VARIATION ALONG THE TAM

The TAM in the Ross Sea Sector are not a simple linear feature. The mountains define a twin arcuate shape (Figure 24) with a major inflection point at the southern end of McMurdo Sound and a minor one near the mouth of the Scott Glacier. The wavelength of these arcs is about 600-800 km. The arcuate shape may be the result of normal intracontinental extension. Frank [1968] suggested that the arcuate shape of island arcs was due to the indentation of a linear feature on a spherical shell. This may be true for linear extension zones, in which case an arcuate shape rather than a linear shape would be expected. Bosworth [1985] noted that the major faults of continental rifts follow curvilinear patterns in plan view defining a subbasin relief that repeats generally every 50-150 km. He gives examples from the Red Sea, the Gregory rift, and the White Nile rift and noted that curvature is also seen in similar bounding faults in the Basin and Range Province. It is possible that such features could also occur on a larger scale as observed in the TAM. The inflection point at McMurdo Sound is, however, more likely to be the result of movement along a major transfer fault up or near the Skelton Glacier. Dextral movement, similar to that postulated up the Byrd Glacier (see below), may have caused the break in the otherwise nearly smooth outline of the coast between northern Victoria Land and the Queen Maud Mountains. Lucchitta et al. [1987] note a conspicuous lineation on a processed Landsat image of the McMurdo Sound and Dry Valleys area. This lineation is just north of the Skelton Glacier and trends WNW-ESE through the Royal Society Range and Koettlitz Glacier and then most likely continues through Mount Discovery and along Minna Bluff. It is possible that this is the major structure (a continental transfer fault or accommodation zone) causing the inflection in the coastline and providing a conduit for volcanic products. Etheridge et al. [1985] described transfer faults as being not simple strike-slip faults but rather accommodation structures analogous to oceanic transforms, in that they allow variations in the geometry of extension along the strike of a rift. Major normal faults can terminate against them (and vice versa) without the necessity for distributed strain throughout the rock mass.

The trend of the basement highs in the Ross Embayment changes from north-south, north of the Byrd Glacier (Figure 24), to northwest-southeast, south of the glacier. This would suggest that the direction of extension, although not necessarily perpendicular to these basement highs, must also change. A major fault is postulated to exist up the Byrd Glacier [Grindley and Laird, 1969]. Grindley [1981] suggested major dextral displacement of the Ross Orogenic belt across this fault and Davey [1981] suggested that an extension of this fault is a transform fault. The fault is, however, more likely to be

another major transfer fault given that this is a continental extension zone. Other transfer faults, perhaps of lesser order, are also likely up the Scott, Beardmore, Nimrod, Koettlitz, Mackay, and David glaciers and possibly many other outlet glaciers. At these transfer faults, longitudinal north-south trending normal faults may terminate, change their spacing, or change the amount of offset. This scenario is similar to that already suggested for longitudinal faults within the TAM Front from Granite Harbour to the Ferrar Glacier, although the transfer faults are likely to be on a smaller scale than up major outlet glaciers. Etheridge [1987] notes that where there is significant oblique slip on normal faults, the transfer faults will also be oblique slip and the fault traces orthogonal. The converse may apply here with north-south trending longitudinal normal faults that presumably delineate the TAM Front near the Byrd Glacier, and perhaps the Skelton Glacier, therefore having oblique slip components. However, there seems to be little likelihood of any strike movement on lesser-order transfer faults, because where normal faults are close to pure dip slip, as they appear to be across the TAM Front in the McMurdo Sound area, the transfer faults are steeply dipping and perpendicular to normal faults [Etheridge, 1987].

The TAM-Ross Embayment system does not appear to change the sense of asymmetry along the rift as seen in many other rifts. The TAM along their entire length define the upper plate, and elements of the Ross Embayment define the lower plate. This suggests that extension was passive. It would therefore seem that the fundamental zone of weakness defined by the Paleozoic fabric of the Ross fold belt was strong enough to ensure that the sense of asymmetry has remained consistent along the entire length of the East Antarctica-West Antarctica boundary in the Ross Sea Sector.

Although there must have been regional variations in the original elevation of the Kukri Peneplain along the length of the TAM corresponding to localized Devonian basins [Barrett, 1981], the elevation of this erosion surface (Figure 24) will mark the relative amount of uplift in any given localized area. The elevation of the peneplain will vary across the extent of the mountains because of the general westerly dip of the mountains under the polar ice cap. However, in areas where the topography and structure are a little more complex, for example between the Beardmore and Nimrod glaciers where three large fault blocks exist across the lateral extent of the TAM, the pattern of peneplain elevations is correspondingly more complex. Likewise, fault blocks separated by transverse or transfer faults need not necessarily have identical tectonic histories. Fault blocks at either end of the TAM may record quite different tectonic events reflecting events within the southwest Pacific, the Ross Embayment, or even the Weddell Embayment. As is suggested on a small scale by the slightly different initiation times of early Cenozoic uplift at Mount England and Mount Doorly, tectonic events along the length of the TAM may even be of a time transgressive nature.

The eastern bulge of northern Victoria Land appears to have complicated the pattern of extension in the Ross Embayment. This is perhaps a result of the accreted Robertson Bay terrane causing bifurcation of the extensional trend of the Victoria Land Basin [Fitzgerald and Gleadow, 1988]. It has been proposed that the Victoria Land Basin and Rennick Graben were originally connected [Cooper et al., 1987; Roland and Tessensohn; 1987] and were subsequently cut off by uplift of the intervening granitic terrane. The uplift of the intervening terrane and the presence of the Robertson Bay terrane possibly caused the axis of extension to shift parallel to the southwest coast of northern Victoria Land. This zone of weakness from Cape Washington to Cape Hallet (Figure 24) is now marked by the presence of late Cenozoic volcanics along the coast and the Polar 3 magnetic anomaly [Bosum et al., 1991] which lies offshore and parallel to the coast.

Acknowledgments. Fieldwork was funded by the New Zealand University Grants Committee through the Antarctic Research Centre of Victoria University of Wellington. Field companions Mark Webster, John Watson, Tony MacPherson, Alex Pyne, and Paul Curry are thanked, as is the New Zealand Antarctic Division and U.S. Navy Squadron VXE-6 for logistic support in the field. R. B. Thompson is thanked for inspiring the naming of Mount Termination. Samples were processed and dated in the Fission Track Laboratory at the University of Melbourne and the project was supported by the Australian Research Grants Scheme and the Australian Institute of Nuclear Science and Engineering. Discussions with Andrew Gleadow, Peter Barrett, Edmund Stump, and Terry Wilson, and comments by Uri ten Brink aided the production of this paper. Nancy Naeser and John Behrendt are thanked for thorough reviews that improved this paper. Sue Selkirk is thanked for assistance with drafting. Support is currently from National Science Foundation grants DPP-8816655 and DPP-8821937.

REFERENCES

Allen, A. D., and G. W. Gibson, Geological investigations in southern Victoria Land, Antarctica, Part 6: Outline of the geology of the Victoria Valley region, *N. Z. J. Geol. Geophys., 5*, 234-242, 1962.

Armstrong, R. L., K-Ar dating: Late Cenozoic McMurdo Volcanic Group and dry valley glacial history, Victoria Land, Antarctica, *N. Z. J. Geol. Geophys., 6*, 685-698, 1978.

Barrett, P.J., Textural characteristics of Cenozoic preglacial and glacial sediments at site 270, Ross Sea, Antarctica, *Initial Rep. Deep Sea Drill. Proj., 28*, 757-767, 1975.

Barrett, P. J., History of the Ross Sea region during the deposition of the Beacon Supergroup 400-180 million years ago, *J. R. Soc. N. Z., 11*, 447-458, 1981.

Barrett, P.J. (Ed.), Antarctic Cenozoic history from the MSSTS-1 drillhole, McMurdo Sound, *DSIR Bull., 237*, 176 pp., 1986.

Barrett, P. J., Oligocene sequence cored at CIROS-1, western McMurdo Sound, *N. Z. Antarct. Rec., 7*(3), 1-7, 1987.

Barron, J., et al., *Proc. Ocean Drill. Program Initial Rep., 119*, 1989.

Behrendt, J. C., and A. K. Cooper, Evidence of rapid Cenozoic uplift of the shoulder escarpment of the Cenozoic West Antarctic rift system, and a speculation on possible climate forcing, *Geology, 19*, 315-319, 1991.

Bennett, D. J., and B. A. Sissons, Gravity models across the Transantarctic Mountain Front near New Harbour, McMurdo Sound, Antarctica, *N. Z. J. Geol. Geophys., 27*, 413-424, 1984.

Bentley, C. R., Crustal structure of Antarctica from geophysical evidence - A review, in *Antarctic Earth Science*, edited by R. L. Oliver, P. R. James, and J. B. Jago, pp. 491-497, Australian Academy of Science, Canberra, 1983.

Berg, J. H., and D. L. Herz, Thermobarometry of two-pyroxene-granulite inclusions in Cenozoic rocks of the McMurdo Sound region, *Antarct. J. U.S., 21*, 19-20, 1986.

Berg, J. H., R. J. Moscati, and D. L. Herz, A petrologic geotherm from a continental rift in Antarctica, *Earth Planet. Sci. Lett., 93*, 98-108, 1989.

Bosum, W., D. Damaske, J. C. Behrendt, and R. Saltus, The aeromagnetic survey of northern Victoria Land and the western Ross Sea during GANOVEX IV and a geophysical-geological interpretation, in *Geological Evolution of Antarctica*, edited by M. R. A. Thomson, J. A. Crame, and J. W. Thomson, pp. 267-272, Cambridge University Press, New York, 1991.

Bosworth, W., Geometry of propagating continental rifts, *Nature, 316*, 625-627, 1985.

Brown, R. W., Backstacking apatite fission-track "stratigraphy": A new method for resolving the erosional and isostatic rebound components of tectonic uplift histories, *Geology, 19*, 74-77, 1991.

Calk, L. C., and C. W. Naeser, The thermal effect of a basaltic intrusion on fission tracks in quartz monzonite, *J. Geol., 81*, 189-198, 1973.

Calkin, P. E., and R. L Nichols, Quaternary studies in Antarctica (review), in *Antarctic Geology and Geophysics*, edited by R. J. Adie, pp. 625-643, Universitetforslaget, Oslo, 1972.

Cooper, A. K., and F. J. Davey, Episodic rifting of Phanerozoic rocks in the Victoria Land

Basin, western Ross Sea, Antarctica, *Science, 229*, 1085-1087, 1985.

Cooper, A. K., F. J. Davey, and J. C. Behrendt, Seismic stratigraphy and structure of the Victoria Land Basin, western Ross Sea, Antarctica, in *The Antarctic Continental Margin: Geology and Geophysics of the western Ross Sea, Earth Sci. Ser.*, vol. 5B, edited by A. K. Cooper and F. J. Davey, pp. 27-65, Cirum-Pacific Council for Energy and Mineral Resources, Houston, Tex., 1987.

Craddock, C. C. (Complier), Geologic Map of Antarctica 1:5,000,000, in *Antarctic Geoscience*, edited by C. C. Craddock, University of Wisconsin Press, Madison, 1982.

Crittenden, M.D., P. J. Coney, and G. H. Davis (Ed.), Tectonic significance of metamorphic core complexes of the North American Cordillera, *Mem. Geol. Soc. Am., 153*, 490 pp., 1980.

Dalziel, I. W. D., and D. H. Elliot, West Antarctica: Problem child of Gondwanaland, *Tectonics, 1*, 3-19, 1982.

Dalziel, I. W. D., S. W. Garrett, A. M. Grunow, R. J. Pankhurst, B. C. Storey, and W. R. Vennum, The Ellsworth - Whitmore Mountains crustal block: Its role in the tectonic evolution of West Antarctica, in *Gondwana Six: Structure, Tectonics and Geophysics, Geophys. Monogr. Ser.*, vol. 40, edited by G. K. McKenzie, pp. 173-182, AGU, Washington D. C., 1987.

Davey, F. J., Geophysical studies in the Ross Sea region, *J. R. Soc. N. Z., 11*, 465-479, 1981.

Davey, F. J., K. Hinz, and H. Schroeder, Sedimentary basins of the Ross Sea, Antarctica, in *Antarctic Earth Science*, edited by R. L. Oliver, P. R. James, and J. B. Jago, pp. 533-538, Australian Academy of Science, Canberra, 1983.

David, T. W. E., and R. E. Priestley, Glaciology, physiography, stratigraphy and tectonic geology of south Victoria Land, *Reports of Scientific Investigations - British Antarctic Expedition 1907-09, Geology 1*, 319 pp, 1914.

Decker, E. R., and G. J. Bucher, Geothermal studies in the Ross Island - Dry Valley region (review), in *Antarctic Geoscience*, edited by C. C. Craddock, pp. 887-894, University of Wisconsin Press, Madison, 1982.

Denton, G.H., M. L. Prentice, D. E. Kellogg, and T. B. Kellogg, Late Tertiary history of the Antarctic ice sheet: Evidence from the Dry Valleys, *Geology, 12*, 263-267, 1984.

Dobson, M. H., Closure temperature in cooling geochronological and petrological systems, *Contrib. Mineral. Petrol., 40*, 259-274, 1973.

Drewry, D. J., Initiation and growth of the East Antarctic ice sheet, *J. Geol. Soc. London, 131*, 255-273, 1975.

Duddy, I. R., P. F. Green, and G. M. Laslett, Thermal annealing of fission tracks in apatite 3: Variable temperature behaviour, *Isot. Geosci., 73*, 25-38, 1988.

Elliot, D. H., Aspects of the evolution of West Antarctica and the Transantarctic Mountains, Abstracts of the Sixth International Gondwana Symposium, Misc. Publ. 231, p. 38, Instit. for Polar Stud., Ohio State Univ., Columbus, 1985.

Etheridge, M. A., The geometry and tectonic significance of transfer faults in continental extension terranes, *Geol. Soc. Aust. Abstr., 19*, 78-79, 1987.

Etheridge, M. A., J. C. Branson, and P. G. Stuart-Smith, Extensional basin-forming structures in Bass Strait and their importance for hydrocarbon exploration, *J. Aust. Petrol. Explor. Assoc., 25*, 344-361, 1985.

Findlay, R. H., D. N. B. Skinner, and D. Craw, Lithostratigraphy and structure of the Koettlitz Group, McMurdo Sound, Antarctica, *N. Z. J. Geol. Geophys., 27*, 513-536, 1984.

Fitzgerald, P. G., Uplift history of the Transantarctic Mountains in the Ross Sea Sector and a model for their formation, Ph.D. dissertation, 327 pp., Univ. of Melbourne, Victoria, Australia, 1987.

Fitzgerald, P.G., and A. J. W. Gleadow, Fission track geochronology, tectonics and structure of the Transantarctic Mountains in northern Victoria Land, Antarctica, *Isot. Geosci., 73*, 169-198, 1988.

Fitzgerald, P.G., and A. J. W. Gleadow, New approaches in fission track geochronology as a tectonic tool: Examples from the Transantarctic Mountains, *Nucl. Tracks, 17*, 351-357, 1990.

Fitzgerald, P. G., M. Sandiford, P. J. Barrett, and A. J. W. Gleadow, Asymmetric extension associated with uplift and subsidence of the Transantarctic Mountains and Ross Embayment, *Earth Planet. Sci. Lett., 81*, 67-78, 1986.

Ford, A. B., and P. J. Barrett, Basement rocks at DSDP Site 270, Ross Sea, Antarctica, *Initial Rep. Deep Sea Drill. Proj., 28*, 861-868, 1975.

Frank, F. C., Curvature of island arcs, *Nature, 220*, 363, 1968.

Gleadow, A. J. W., and C. K. Brooks, Fission track dating, thermal histories and tectonics of igneous intrusions in East Greenland, *Contrib. Mineral. Petrol., 71*, 45-60, 1979.

Gleadow, A. J. W., and I. R. Duddy, A natural long term annealing experiment for apatite, *Nucl. Tracks, 5*, 169-174, 1981.

Gleadow, A. J. W., and P. G. Fitzgerald, Uplift history and structure of the Transantarctic Mountains: New evidence from fission track dating of basement apatites in the Dry Valleys area, southern Victoria Land, *Earth Planet. Sci. Lett., 82*, 1-14, 1987.

Gleadow, A. J. W., B. C. McKelvey, and K. U. Ferguson, Uplift history of the Transantarctic Mountains in the Dry Valleys area, southern Victoria Land, Antarctica, from apatite fission track ages, *N. Z. J. Geol. Geophys., 27*, 457-464, 1984.

Gleadow, A. J. W., I. R. Duddy, P. F. Green, and K. A. Hegarty, Fission track lengths in the apatite annealing zone and the interpretation of mixed ages, *Earth Planet. Sci. Lett., 78*, 245-254, 1986a.

Gleadow, A. J. W., I. R. Duddy, P. F. Green, and J. F. Lovering, Confined fission track lengths in apatite - A diagnostic tool for thermal history analysis, *Contrib. Mineral. Petrol., 94*, 405-415, 1986b.

Gould, L. M., Structure of the Queen Maud Mountains, Antarctica, *Geol. Soc. Am. Bull., 46*, 973-984, 1935.

Grapes, R. H., D. L. Reid, and J. G. McPherson, Shallow dolerite intrusion and phreatic eruption in the Allan Hills region, Antarctica, *N. Z. J. Geol. Geophys., 17*, 563-577, 1974.

Green, P. F., A new look at statistics in fission track dating, *Nucl. Tracks, 5*, 77-86, 1981.

Green, P. F., Comparsion of zeta calibration baselines for fission-track dating of apatite, zircon and sphene, *Chem. Geol., 58*, 1-22, 1985.

Green, P. F., On the thermo-tectonic evolution of Northern England: evidence from fission track analysis, *Geol. Mag., 123*, 493-506, 1986.

Green, P. F., I. R. Duddy, A. J. W. Gleadow, P. T. Tingate, and G. M. Laslett, Thermal annealing of fission tracks in apatite: 1 - A qualitative description, *Isot. Geosci., 59*, 237-253, 1986.

Green, P. F., I. R. Duddy, G. M. Laslett, K. A. Hegarty, A. J. W. Gleadow, and J. F. Lovering, Thermal annealing of fission tracks in apatite 4. Quantitative modelling techniques and extension to geological timescales, *Isot. Geosci., 79*, 155-182, 1989.

Grindley, G. W., The geomorphology of the Miller Range, Transantarctic Mountains, with notes on the glacial history and neotectonics of East Antarctica, *N. Z. J. Geol. Geophys., 10*, 557-598, 1967.

Grindley, G. W., Precambrian rocks of the Ross Sea region, *J. R. Soc. N. Z., 11*, 411-423, 1981.

Grindley, G. W., and M. G. Laird, Geology of the Shackleton Coast, in *Geological Maps of Antarctica, Antarct. Map Folio Ser.*, folio 12, edited by C. C. Craddock, Am. Geogr. Soc., New York, 1969.

Grindley, G. W., V. R. McGregor, and R. I. Walcott, Outline of the geology of the Nimrod-Beardmore-Axel Heiberg Glaciers region, Ross Dependency, in *Antarctic Geology*, edited by R. J. Adie, pp. 206-219, North-Holland, New York, 1964.

Gunn, B. M., Geological structure and correlation in Antarctica, *N. Z. J. Geol. Geophys., 6*, 423-443, 1963.

Gunn, B. M., and R. I. Walcott, The geology of the Mt. Markham region, Ross Dependency, Antarctica, *N. Z. J. Geol. Geophys., 5*, 407-426, 1962.

Gunn, B. M., and G. Warren, Geology of Victoria Land between the Mawson and Mulock Glaciers, Antarctica, *Bull. N. Z. Geol. Surv., 71*, 157 pp., 1962.

Haack, U., The closing temperature for fission track retention in minerals, *Am. J. Sci., 277*, 459-464, 1977.

Hamilton, W., New interpretation of Antarctic tectonics, *U.S. Geol. Surv. Prof. Pap., 400B*, 379-380, 1960.

Hamilton, W., Tectonics of Antarctic, in The Backbone of the America's: Tectonic History from Pole to Pole, A Symposium, *Am. Assoc. Pet. Geol. Mem.*, 2, 4-15, 1963.

Hamilton, W., Tectonics of Antarctica, *Tectonophysics, 4*, 555-568, 1967.

Hamilton, W., and P. T. Hayes, Geology of the Taylor Glacier - Taylor Dry Valley region, south Victoria Land, Antarctica, *U.S. Geol. Surv. Prof. Pap., 400B*, 376-378, 1960.

Hamilton, W., P. T. Hayes, R. Calvert, V. C. Smith, S. D. Elmore, P. R. Barnett, and N. Conklin, Diabase sheets of the Taylor Glacier region, Victoria Land, Antarctica, *U.S. Geol. Surv. Prof. Pap., 456B*, 71 pp., 1965.

Harrison, T. M., R. L. Armstrong, C. W. Naeser, and J. E. Harakal, Geochronology and thermal history of the Coast Plutonic complex, near Prince Rupert, B.C., *Can. J. Earth Sci., 16*, 400-410, 1979.

Harwood, D., Diatoms, in Antarctic Cenozoic History From the MSSTS-1 Drillhole, McMurdo Sound, edited by P. J. Barrett, *DSIR Bull., 237*, 69-90, 1986.

Haskell, T. R., Thermal metamorphism of Beacon Group sandstone of the Taylor Valley, Antarctica, *Nature, 201*, 910, 1964.

Haskell, T. R., J. P. Kennett, W. Prebble, G. Smith, and I. A. G. Willis, The geology of the middle and lower Taylor Valley of southern Victoria Land, Antarctica, *Trans. R. Soc. N. Z., Geol., 2*, 169-186, 1965.

Hayes, D. E., and F. J. Davey, Geophysical study of the Ross Sea, Antarctica, *Initial Rep. Deep Sea Drill. Proj., 28*, 887-908, 1975.

Hayes, D. E., et al., *Initial Rep. Deep Sea Drill. Proj., 28*, 1017 pp., 1975.

Hinz, K., and M. Block, Results of geophysical investigations in the Weddell Sea and in the Ross Sea, Antarctica: Exploration in New Regions, 11th World Pet. Congr., vol. PD 2(1), pp. 1-3, Wiley, London, 1983.

Hurford, A. J., and P. F. Green, The zeta age calibration of fission track dating, *Isot. Geosci., 1*, 285-317, 1983.

Jankowski, E. J., and D. J. Drewy, The structure of West Antarctica from geophysical studies, *Nature, 291*, 17-21, 1981.

Katz, H. R., Post-Beacon tectonics in the region of Amundsen and Scott Glaciers, Queen Maud Range, Transantarctic Mountains, in *Antarctic Geoscience*, edited by C. C. Craddock, pp. 827-834, University of Wisconsin Press, Madison, 1982.

Kerr, R. A., Ice cap of 30 million years ago detected, *Science, 224*, 141-142, 1984.
King, B. C., Geological relationships between South Africa and Antarctica, *Alex. L. du Toit Mem. Lect., 9*, 32 pp., 1965.
Kyle, P. R., and J. W. Cole, Structural controls of volcanism in the McMurdo Volcanic Group, McMurdo Sound, Antarctica, *Bull. Volcanol., 38*, 16-35, 1974.
Kyle, P. R., D. H. Elliot, and J. F. Sutter, Jurassic Ferrar Group tholeiites from the Transantarctic Mountains, Antarctica and their relationship to the initial fragmentation of Gondwana, in *Gondwana Five*, edited by M. M. Cresswell and P. Vella, pp. 283-287, A.A. Balkema, Rotterdam, 1981.
Laird, M. G., Geomorphology and stratigraphy of the Nimrod Glacier - Beaumont Bay region, south Victoria Land, Antarctica, *N. Z. J. Geol. Geophys., 6*, 465-484, 1963.
Laslett, G. M., W. S. Kendall, A. J. W. Gleadow, and I. R. Duddy, Bias in measurement of fission-track length distributions, *Nucl. Tracks, 6*, 79-85, 1982.
Laslett, G. M., A. J. W. Gleadow, and I. R. Duddy, The relationship between fission track length and density in apatite, *Nucl. Tracks, 9*, 29-38, 1984.
Laslett, G. M., P. F. Green, I. R. Duddy, and A. J. W. Gleadow, Thermal modelling of fission tracks in apatite: 2. A quantitative analysis, *Chem. Geol., 65*, 1-13, 1987.
LeMasurier, W. E., and J. W. Thomson (Eds.), *Volcanoes of the Antarctic Plate and Southern Oceans, Antarct. Res. Ser.*, vol. 48, 487 pp., AGU, Washington, D. C., 1990.
Lister, G. S., M. A. Etheridge, and P. A. Symonds, Application of the detachment fault model to the formation of passive continental margins, *Geology, 14*, 246-250, 1986.
Lopatin, B. G., Basement complex of the McMurdo "oasis", south Victoria Land, in *Antarctic Geology and Geophysics*, edited by R. J. Adie, pp. 287-292, Universitetforslaget, Oslo, 1972.
Lucchitta, B. K., J. A. Bowell, K. L. Edwards, E. M. Eliason, and H. M. Ferguson, Multispectral Landsat Images of Antarctica, *U. S. Geol. Surv. Bull.*, 1696, 21 pp., 1987.
McGinnis, L. D., D. D. Wilson, W. J. Burdelik, and T. H. Larsen, Crust and upper mantle study of McMurdo Sound, in *Antarctic Earth Science*, edited by R. L. Oliver, P. R. James, and J. B. Jago, pp. 204-208, Australian Academy of Science, Canberra, 1983.
McGregor, V. R., Geology of the area between the Axel Heiberg and Shackleton Glaciers, Queen Maud Range, Antarctica. Part 1 - Basement complex, structure and glacial geology, *N. Z. J. Geol. Geophys., 8*, 314-343, 1965.
McKelvey, B. C., and P. N. Webb, Geological investigations in southern Victoria Land, Antarctica, Part 3. Geology of Wright Valley, *N. Z. J. Geol. Geophys., 5*, 143-162, 1962.
McKelvey, B.C., P. N. Webb, D. M. Harwood, and M. C. G. Mabin, The Dominion Range Sirius Group - A record of the Late Pliocene-Early Pleistocene Beardmore Glacier, in *Geological Evolution of Antarctica*, edited by M. R. A. Thomson, J. A. Crame, and J. W. Thomson, pp. 675-682, Cambridge University Press, New York, 1991.
Mercer, J. H., When did open marine conditions last prevail in the Wilkes and Pensacola Basins, East Antarctica and when was the Sirius Formation emplaced, *S. Afr. J. Sci., 81*, 241-243, 1985.
Mercer, J. H., Southernmost Chile: A modern analog of the southern shores of the Ross Embayment during Pliocene warm intervals, *Antarct. J. U.S., 21*(5), 103-105, 1986.
Miagkov, S. M., Relief development of the dry valley region, Victoria Land, *Antarct. J. U.S., 8*, 37-40, 1973.
Moore, M. E., A. J. W. Gleadow, and J. F. Lovering, Thermal evolution of rifted continental margins: New evidence from fission tracks in basement apatites from southeastern Australia, *Earth Planet. Sci. Lett., 78*, 255-270, 1986.
Murtaugh, J. G., Geology of the Wisconsin Range Batholith, Transantarctic Mountains, *N. Z. J. Geol. Geophys, 12*, 526-550, 1969.
Naeser, C. W., The fading of fission-tracks in the geologic environment - data from deep drill holes (abstract), *Nucl. Tracks, 5*, 248-250, 1981.
Naeser, C. W., and H. Faul, Fission track annealing in apatite and sphene, *J. Geophys. Res., 74*, 705-710, 1969.
Naeser, C. W., B. Bryant, M. D. Crittenden, and M. L. Sorensen, Fission-track ages of apatite in the Wasatch Mountains, Utah: An uplift study, *Geol. Soc. Am. Mem., 157*, 29-36, 1983.
Palmer, K., X.R.F. of granitoids and associated rocks from south Victoria Land, Antarctica, *Antarct. Data Ser., no. 13.*, 26 pp., Geol. Dep., Victoria Univ. of Wellington, N. Z., 1987.
Priestley, R. E., and T. W. E. David, Geological notes of the British Antarctic Expedition, 1907-09, *Proceeding of the 11th International Geological Congress, Stockhom*, vol. 2, pp. 767-811, 1912.
Robertson, J. D., C. R. Bentley, J. H. Clough, and L. L. Greischer, Seabottom topography and crustal structure below the Ross Ice Shelf, Antarctica, in *Antarctic Geoscience*, edited by C. C. Craddock, pp. 1083-1090, University of Wisconsin Press, Madison, 1982.
Robinson, E. S., Geologic structure of the Transantarctic Mountains and adjacent ice covered areas, Ph.D dissertation, 292 pp., Univ. of Wisconsin, Madison, 1964.
Roland, N. W., and F. Tessensohn, Rennick faulting - An early phase of Ross Sea Rifting, in *German Antarctic North Victoria Land Expedition 1982/83 Ganovex III*, vol. 2, edited by F. Tessensohn and N. W. Roland, pp. 275-302, Bundesanstalt fur Geowissenschaften und Rohstoffe, Stuttgard, 1987.
Rosendahl, B. R., Architecture of continental rifts with special reference to East Africa, *Annu. Rev. Earth. Planet. Sci., 15*, 445-503, 1987.
Schmidt, D. L., and P. D. Rowley, Continental rifting and transform faulting along the Jurassic Transantarctic rift, Antarctica, *Tectonics, 5*, 279-291, 1986.
Schopf, J. M., Ellsworth Mountains: Position in West Antarctica due to sea-floor spreading, *Science, 164*, 63-66, 1969.
Seiber, K. G., Compositional variation in apatites, B.Sc.(Hons.) dissertation, 85 pp., Geol. Dep., Univ. of Melbourne, Victoria, Australia, 1986.
Skinner, D. N. B., A summary of the geology of the region between Byrd and Starshot Glaciers, southern Victoria Land, in *Antarctic Geology*, edited by R. J. Adie, pp. 284-292, North-Holland, New York, 1964.
Skinner, D. N. B., The granites and two orogenies of southern Victoria Land, in *Antarctic Earth Science*, edited by R. L. Oliver, P. R. James, and J. B. Jago, pp. 160-163, Australian Academy of Science, Canberra, 1983.
Skinner, D. N. B., and J. Ricker, Geology of the region between the Mawson and Priestley Glaciers, north Victoria Land, Antarctica: Part 1 Basement metasedimentary and igneous rocks, *N. Z. J. Geol. Geophys., 11*, 1009-1040, 1968a.
Skinner, D. N. B., and J. Ricker, Geology of the region between the Mawson and Priestley Glaciers, north Victoria Land, Antarctica: Part 2 Upper Paleozoic to Quaternary geology, *N. Z. J. Geol. Geophys., 11*, 1041-1075, 1968b.
Smith, A. G., and D. J. Drewry, Transantarctic uplift: Delayed phase change due to a linear heat source, *Nature, 309*, 536-538, 1984.
Smithson, S. B., Gravity interpretation in the Transantarctic Mountains near McMurdo Sound, Antarctic, *Geol. Soc. Am. Bull., 83*, 3437-3442, 1972.
Stern, T. A., and U. S. ten Brink, Flexural uplift of the Transantarctic Mountains, *J. Geophys. Res., 94*(B8), 10315-10330, 1989.
Stump, E., M. F. Sheridan, S. G. Borg, and J. F. Sutter, Early Miocene subglacial basalts, the East Antarctic Ice Sheet, and the uplift of the Transantarctic Mountains, *Science, 207*, 757-759, 1980.
Stump, E., R. J. Korsch, and D. G. Edgerton, The myth of the Nimrod and Beardmore Orogenies, in *Geological Evolution of Antarctica*, edited by M. R. A. Thomson, J. A. Crame, and J. W. Thomson, pp. 143-147, Cambridge University Press, New York, 1991.
Tingey, R. J., Uplift in Antarctica, *Z. Geomorphol. N.F. Suppl., 54*, 85-99, 1985.
Torii, T., A review of the Dry Valley Drilling Project, 1971-76, *Polar Rec., 20*, 533-541, 1981.
Voronov, P. S., Tectonics and neotectonics of Antarctica, in *Antarctic Geology*, edited by R. J. Adie, pp. 692-700, North-Holland, New York, 1964.
Wagner, G. A., and G. M. Reimer, Fission track tectonics: The tectonic interpretation of fission track apatite ages, *Earth Planet. Sci. Lett., 14*, 263-268, 1972.
Wagner, G. A., G. M. Reimer, and E. Jager, The cooling ages derived by apatite fission track, mica Rb-Sr, and K-Ar dating: The uplift and cooling history of the Central Alps, *Mem. 30*, 27 pp., Inst. Geol. Mineral., Univ. of Padova, Italy, 1977.
Wagner, G. A., A. J. W. Gleadow, and P.G. Fitzgerald, The significance of the partial annealing zone in apatite fission-track analysis: Projected track length measurements and uplift chronology of the Transantarctic Mountains, *Isot. Geosci., 79*, 295-305, 1989.
Warren, G, Geology of the Terra Nova Bay - McMurdo Sound area, Victoria Land, *Antarct. Map Folio Ser., Plate 13*, folio 12, Geology, Am. Geogr. Soc., New York, 1969.
Webb, P. N., Wright Fjord, Pliocene marine invasion of an Antarctic Dry Valley, *Antarct. J. U.S., 7*, 227-234, 1972.
Webb, P. N., Foraminifera (Late Cenozoic), in Antarctic Cenozoic History From the MSSTS-1 Drillhole, McMurdo Sound, edited by P. J. Barrett, *DSIR Bull., 327*, 127-130, 1986.
Webb, P. N., and J. H. Wrenn, Upper Cenozoic micropaleontology and biostratigraphy of eastern Taylor Valley, Antarctica, in *Antarctic Geoscience*, edited by C. C. Craddock, pp. 1117-1122, University of Wisconsin Press, Madison, 1982.
Webb, P. N., D. M. Harwood, B. C. McKelvey, J. H. Mercer, and L. D. Stott, Cenozoic marine sedimentation and ice volume variation on the East Antarctic craton, *Geology, 12*, 287-291, 1984.
Webb, P. N., B. C. McKelvey, D. M. Harwood, M. C. G. Mabin and J. H. Mercer, Sirius Formation of the Beardmore Glacier Region, *Antarct. J. U.S., 22*(1/2), 8-13, 1987.
Wellman, P., and R. J. Tingey, Glaciation, erosion and uplift over part of East Antarctica, *Nature, 291*, 142-144, 1981.
Wilch, T. I., D. R. Lux, W. C. McIntosh, and G. H. Denton, Plio-Pleistocene uplift of the McMurdo Dry Valley sector of the Transantarctic Mountains, *Antarct. J. U.S., 24*(5), 30-33, 1989.
Wrenn, J.H., and P. N. Webb, Physiographic analysis and interpretation of the Ferrar Glacier - Victoria Valley area, Antarctica, in *Antarctic Geoscience*, edited by C. C. Craddock, pp. 1091-1100, University of Wisconsin Press, Madison, 1982.

P. G. Fitzgerald, Department of Geology, Arizona State University, Tempe, AZ 85287-1404.

(Received August 16, 1990;
revised August 7, 1991;
accepted September 17, 1991.)